国際化推進共同研究概要

No. 1

タイトル: Effects of charged particle irradiations on the microstructure and mechanical properties of reactor pressure vessel steels

研究代表者: ODETTE, George, Robert

所内世話人: 渡辺 英雄

実 施 期 間: 2014 年 10 月 5 日～ 10 月 19 日

研究概要：

鉄系原子力用構造材料の照射環境下での脆化挙動解明を目的として、イオン並びに電子線照射を炉の使用温度にて実施した。ナノインデンター硬さ測定、TEM(九大)及びアトムポローブ(UCSB)による観察から、高損傷速度で特有なカスケード内形成型欠陥の寄与をモデル化し、これと点欠陥再結合率の変化に起因する照射速度効果の補正を適用する事により、イオン照射実験結果から中性子照射における照射硬化を評価できた。

Effects of charged particle irradiations on the microstructure and mechanical properties of reactor pressure vessel steels

Takuya Yamamoto, Peter Wells, Yuan Wu, G. Robert Odette (University of California Santa Barbara), Hideo Watanabe, Takahiro Onishi (Kyushu University)

Introduction

Safe operation of light water reactors requires accurate prediction of the pressure vessel steel embrittlement typically characterized by a transition temperature shift (TTS). Modeling embrittlement trend curve (ETC) needs in part utilizing data from accelerated irradiations in higher flux test reactors. However, flux influences the various hardening features and corresponding TTS for a given alloy, irradiation temperature and fluence. Indeed, there is evidence that a significant population of transient defect features is important at high flux. These transient features presumably formed within a so-called displacement cascade (a series of displacement reactions creating locally concentrated point defects and those clusters) may: 1) by itself contribute to irradiation hardening and embrittlement; 2) act as defect sinks to enhance point defect recombination to delay (shift to higher fluence) diffusion driven growth of other features contributing hardening and embrittlement; as well as 3) accelerate nucleation of those features. These opposite roles make the flux effects very complicated. Hence, the purpose of the research is to better understand the flux effects including the roles of transient features on microstructural evolutions and radiation induced hardening under three types of – electron (no cascade forming higher flux), Fe ion (high flux with cascades) and neutron (low flux with cascades) – irradiations.

Experimental procedure

Three A533B steels with different Cu levels were used in this study, which are referred to as LG without Cu, LH with 0.11 wt% Cu, and LI with 0.20 wt% Cu. The specimens for ion irradiation and in situ observation via HVEM were annealed (austenitized) at 900 °C for 1 h, air cooled, tempered at 664 °C for 4 h, air cooled, stress relieved at 600 °C for 40 h, and air cooled. Ion irradiation with 2.4 MeV Fe^{2+} was conducted in the temperature range from room temperature to 350 °C using the tandem accelerator at Kyushu University. Hardness tests were conducted at room temperature before and after ion irradiation using an Elionix ENT-1100 nano-indenter with a load of 1 gf. A triangular pyramidal diamond indenter (Berkovich type) with a semi-apex angle of 65° was used. For the LI sample, atom probe tomography (APT) was also conducted after ion irradiation to 1 dpa at 290°C and 350°C. The atom probe samples were run in a LEAP 3000 HR at the University of California, Santa Barbara in voltage mode using a pulse fraction of 20% and specimen temperature of 50K.

Electron irradiation was performed using 1.0 MeV electrons and a high voltage electron microscope (JEM-1000) in the HVEM Laboratory at Kyushu University. Electron irradiation was conducted at 290 °C and 350 °C. at a lower dpa dose rate of 2.5×10^{-5} dpa/s to create an irradiated area large enough for sampling APT specimens. Mechanical and electro-polishing and focused ion beam (FIB) machining were employed to prepare each transparent HVEM sample with a rectangular notch as a landmark for target location. Irradiations to achieve displacement damage levels from 0.1 to 0.4 dpa were performed at a temperature of 290 °C near the landmark. The irradiated regions were approximately 10 μm in diameter, and the specimens were approximately 200 nm in thickness. FIB machining was then employed to prepare APT samples from the irradiated regions.

Results and Discussion

The dose dependence of the radiation-induced hardness of alloys with different Cu levels after irradiation up to 1.0 dpa at room temperature (RT) and at 290 °C is shown in Figs. 1 (a) and (b), respectively. Here, radiation-induced hardness is defined by the difference in the hardness before and after irradiation, $\Delta H = H_{irrad} - H_{unirrad}$. The indentation measurements were performed before and after irradiation using the same samples. At both irradiation temperatures, that start of irradiation led a rapid rise in radiation-induced hardening, that became nearly saturated once at approximately 0.1 dpa but followed by gradual increase with dose.

Figure 1(c) shows the ion induced hardening trends of the three alloys (yield stress change, $\Delta\sigma_y$, converted from ΔH) compared with the corresponding trends in IVAR experiment in a test reactor at much lower dose rate of $\approx 10^{-9}$ dpa/s. In IVAR condition significant Cu dependence was observed even at the lowest $\approx 2 \times 10^{-4}$ dpa so that the high-Cu LI shows ≈ 80 MPa larger hardening than no-Cu LG, which is actually caused by Cu-riched precipitates (CRP), whereas the ion irradiation hardening has no Cu effect in that dose range suggesting no CRP formation. TEM observation suggested there is no visible loops or precipitates in the low dose range. Never the less, the ion irradiation induced hardening in the range is as large as the high-Cu LI in IVAR, that can be attributed to hardening caused by the transient feature as was mentioned above.

Under the very high dose rate in ion irradiation, there is no time for transient features to recover, but the type of defects can quickly fill the space leading to a saturated hardening. Since the transiency has not been confirmed (or does not even matter for the saturation) we call these simply Cascade Fragments (CF). The CF hardening can explain the initial rapid rise and saturation in hardening regardless the T_{irr} or Cu content as shown in Figure 2a. The CF hardening forms a base hardening as is observed in no-Cu LG, while in higher Cu alloys additional hardening is observed at high dose. Figure 3c plots the additional part of hardening (total subtracted by CF $\Delta\sigma_y$) with dose compared with IVAR. Note, CF hardening is negligible at the low dose rate IVAR condition. Figure 3b clearly indicates that CRP hardening is significantly delayed in ion irradiation as is expected due to enhanced point defect recombination at high dose rate. This type of flux effects can be adjusted by using an effective dose given by an actual dose multiplied by a flux scaling factor $(\phi_r/\phi)^p$, where p depends on flux effect mechanisms and changes between 0 and 1, but $p \approx 0.25$ is commonly found to work for wide range. Figure 3c plots the same $\Delta\sigma_y$ in an effective dose scale with p=0.25. The CRP hardening trends in ion and IVAR irradiation surprisingly merges on this scale.

Microstructural evolutions in the three types of irradiations observed to date are also different one another presumably due to the delay at high dose rate in ion and electron irradiations as well as to the lack of CF in electron irradiation. We continue atom probe tomography and TEM observation of the alloys for further studies.

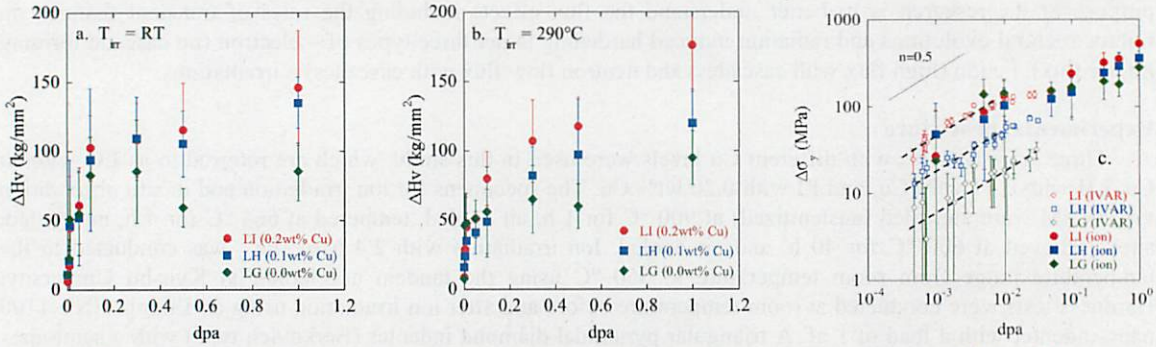

Figure 1 Dose dependence of irradiation hardening, ΔH, at a) room temperature and b) 290°C; c) Converted yield stress change ($\Delta\sigma_y$) compared with IVAR irradiation experiment in a test reactor at much lower dose rate .

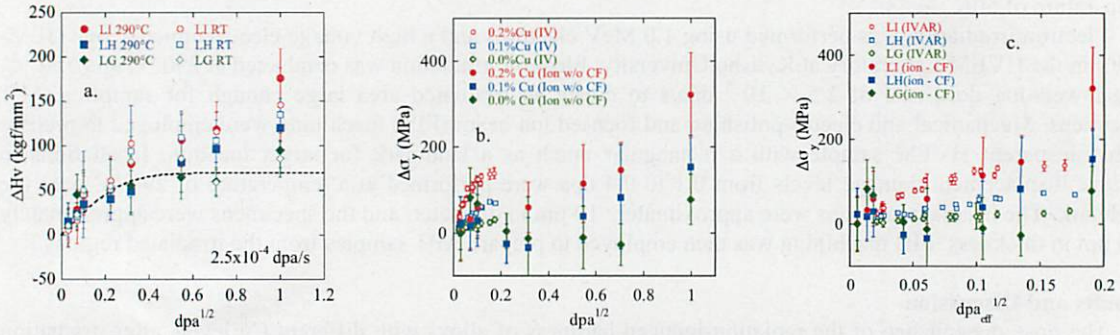

Figure 2 a) Dose dependence of irradiation hardening, ΔH, in ion irradiation at RT and 290°C with a model hardening due to cascade fragments; Comparison of ion induced hardening subtracted by the model CF $\Delta\sigma_y$ as a function of b) actual dose and c) effective dose that considers high dose rate recombination effects (p=0.25).

Summary

Ion irradiated 0.8Ni-1.4Mn-0.5Si RPV alloys with varied Cu of 0 to 0.2 % showed very rapid hardening that does not depend on irradiation temperature or Cu level. This hardening can be attributed to cascade induced defect complex, or cascade fragments (CF). CRP hardening under ion irradiation is significantly delayed compared to IVAR test reactor condition presumably due to enhanced recombination at $\approx 10^6$ higher dose rate. The delaying effects are, however, surprisingly adjusted by subtraction of CF hardening and a well known flux scaling using $(\phi_r/\phi)^p$, where $p \approx 0.25$.

Acknowledgements

Part of the research performed by UC Santa Barbara participants is supported by US DOE.

国際化推進共同研究概要

No. 2

タイトル: Towards high mode purity in ECRH transmission lines for ITER.

研究代表者: KASPAREK, Walter, Hermann

所内世話人: 出射 浩

実 施 期 間: 2015 年 2 月 22 日 ～ 27 日、3 月 3 日 ～3 月 5 日

研究概要 :

ITER における高効率大電力伝送には、主伝送モードから高次不要モードの励起が問題となる。高次不要モードはアーキング、過熱といった問題を引き起こす。高次モード励起を実験的に精査するため、高純度主モード励起が必要となる。主モード励起はこれまで 96%励起にとどまっていた。そのため、共振器を用いたモード発生器が提案されたが 94%励起に留まっている。新たに2つのガウスビームを合成する手法を考案し、理論的に 99.9 % を超える高純度モード励起が行えることを示し、実験的にも 98%励起に成功した。ITER での MHD 不安定性の安定化に用いられる高速ミリ波切替器を2周波数で動作させる方式を検討・提案した。

Towards high mode purity in ECRH transmission lines for ITER

Applicant: Walter Kasparek
Institute of Interfacial Process Engineering and Plasma Technology (IGVP)

Electron Cyclotron Heating (ECH) using high power millimeter waves is an attractive method for plasma production, auxiliary heating, and current drive in a nuclear fusion research. In planned fusion experiments at the International Thermonuclear Experimental Reactor (ITER), the injected ECH will have a total power of 20 MW at an operating frequency of 170 GHz. For the 20 MW injection, high power gyrotron oscillators of 24 MW will be prepared. The output beam from each gyrotron oscillator is led to a Circular Corrugated (CC) waveguide line, and transmitted as an HE_{11} mode of a main eigen-mode in the waveguide. Twenty CC waveguide lines will be prepared to transmit the total 20 MW power. Excitation of unwanted higher-order modes in the oversized waveguide causes some problems such as remarkable transmission losses and arcing. Transmission losses in the ITER ECH system have been estimated, including the higher-order mode excitation due to misalignment of the transmission components.

This collaboration has been established to excite and transmit the high-purity main HE_{11} mode under monitoring and controlling of the transmitted wrong modes for the CW high power application.

The International Joint Research team consisted (besides the applicant) of Hiroshi Idei (RIAM, Kyushu), Keishi Sakamoto (JAEA Naka), Takashi Shimozuma (NIFS, Toki), Richard Temkin (MIT PSFC Cambridge), Michael Shapiro (MIT PSFC Cambridge), Carsten Lechte (IGVP Stuttgart), and Burkhard Plaum (IGVP Stuttgart).

HE_{11} Mode Generator

The high purity HE_{11} mode exciter is required for comprehensive studies on mode excitation and effects of misalignment in the Circular Corrugated (CC) waveguide transmission. It has been developed for studies in various millimeter-wave applications with the CC waveguide, as well as in the ITER ECH system.

A previous HE_{11} mode exciter based on quasi-optical concepts, which is composed of a corrugated horn, a dielectric focusing lens and millimeter-wave absorber, reached a mode purity of only 0.96. A resonator system to excite the HE_{11} -mode was also investigated. Here, an open cavity consisting of a phase-inverting mirror matched to the HE_{11} mode radiation and a plane semitransparent output mirror was used. The HE_{11} mode was selectively excited in this resonator system. An HE_{11} mode purity of 0.97 was attained. Further experiments on a 170 GHz folded resonator showed that cleaning of an input radiation with an HE_{11} purity of only 65% was possible to an output purity of 94 %. With high-quality resonators, this value could be strongly increased, however, at the expense of the efficiency. It was concluded, that the resonator concept exhibits severe drawbacks when using it in a test facility.

Therefore, for improved performance, an HE_{11} mode exciter using two Gaussian beams has been designed and is described here.

A Gaussian beam has been considered as one of proper coupling beams into the CC waveguides at the HE_{11} mode. The Gaussian amplitude profile is bell-shaped, and the phase is flat at the waist point, showing good similarity for the HE_{11} mode properties. Figure 1 shows radial amplitude profiles of HE_{11} mode and Gaussian beam optimized for coupling into the CC waveguide. Here, the radius of the CC waveguide a is 0.03175 m. The HE_{11} mode amplitude profile is described as J_0 (2.405 r/a), where J_0 is the 0-th order Bessel function of the first kind. Here, the argument of the J_0 function is described with a first zero-crossing solution of 2.405, and the radial r coordinate of the waveguide cross-section. Major differences between the HE_{11} mode and Gaussian profiles are the broadness and the waveguide-edge amplitude. The HE_{11} mode profile is broader, but has zero amplitude at the waveguide edge, r = a. Beam sizes expressed by second central moments are $0.660a$ and $0.645a$ for the HE_{11} mode and the optimized Gaussian distributions, respectively. If a Gaussian beam with larger beam size was considered, core parts of Gaussian and HE_{11} mode amplitude profiles preferably matched together with, while the Gaussian edge amplitude became large. The optimized Gaussian beam size was determined from a balance of the opposing properties on the beam size. Kurtoses of 4-th central moments were 2.5 and 3.0 for the HE_{11} mode and the optimized Gaussian distributions, indicating the Gaussian profile was more peaked than that of the HE_{11} mode. High purity (>0.98) excitation of the HE_{11} mode was intrinsically impossible by a Gaussian beam as indicated in different peakedness or kurtosis of the beams.

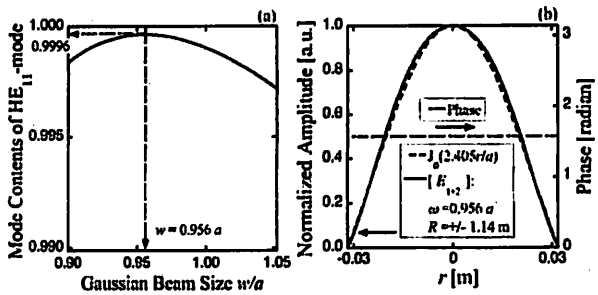

FIG.1: (a) Dependence of matching coefficient between the HE_{11} mode and Gaussian beams on the beam size w. The phase front curvatures R were fixed at 1.143 m (= ka^2 / π). (b) Amplitude and phase profiles for the HE_{11} mode and optimized Gaussian beams at $w = 0.956a$.

The amplitude profiles can be controlled by phase interference in multiple beams with phased-array concept. Therefore, a two-Gaussian-beam system was considered to control the amplitude profile by phase interference. The edge zero-amplitude property was easily obtained by [0, π] phasing at $r = a$ of the two beams combined. Two beam distributions of $E_1(r)$ and $E_2(r)$ were considered for the [0, π] phasing as follows:

$$E_1(r) = E_r(r)\exp\left[j\left(\phi_0 + \frac{\pi r^2}{2a^2}\right)\right],\ E_2(r) = E_r(r)\exp\left[j\left(\phi_0 - \frac{\pi r^2}{2a^2}\right)\right],$$

where $E_r(r)$ was a common radial amplitude profile of the two beams. The two beams with $E_1(r)$ and $E_2(r)$ should be focusing and expanding Gaussian beams with a central phase offset ϕ_0 and phase front curvatures (+/-) R = (+/-) ka^2 / π, provided that $E_r(r)$ was expressed as : $E_r(r) = E_{r0}(r)$ exp ($-r^2 / w^2$) with central amplitude $E_{r0}(r)$ and beam size w. Here k is the wavenumber of the operating 170 GHz frequency. The combined beam profile $E_{1+2}(r)$ (= $E_1(r) + E_2(r)$) can be expressed as:

$$E_{1+2}(r) = 2\,E_r(r)\cos\left(\frac{\pi r^2}{2a^2}\right)\exp(j\phi_0) = 2\,E_{0r}\exp(-r^2/w^2)\cos\left(\frac{kr^2}{2R}\right)\exp(j\phi_0),$$

indicating an amplitude profile of $E_r(r) = E_{r0}(r) \exp(-r^2/w^2) \cos(\pi r^2/2a^2)$ and flat phase of ϕ_0 over the entire profile. The flat phase profile can be considered in the combined beam with the $[0, \pi]$ phasing at $r = a$, which are two key properties of the phase profile to excite the HE_{11} mode. Figure 1(a) shows the matching coefficient between the HE_{11} mode and the combination of Gaussian beams as function of the beam size w. If the matching coefficient is unity, the profiles are identical. High purity of the HE_{11} mode of 0.9996 was obtained at $w = 0.956a$. The phase front curvatures R were fixed at 1.143 m ($=ka^2/\pi$). Figure 1(b) shows the amplitude and phase profiles for the HE_{11} mode and optimized Gaussian beams at $w = 0.956a$. The phase profiles were essentially flat in the combined beam as well as in the HE_{11} mode beam.

This means that in the two-Gaussian-beam system, the HE_{11} mode can be excited at almost 100% in the ideal situation. An experimental setup was designed for the two-Gaussian- beam system; Figure 2 shows a schematic. The system is composed of a corrugated horn antenna, several quasi-optical mirrors, and beam splitters/ combiners. First a Gaussian beam is prepared with a corrugated horn and a phase matched focusing mirror. A second mirror directs the Gaussian beam - at 45 degree linear polarization - to a wire grid polarizer, where it is split into two beams. The phase profiles of the two beams are then formed by combinations of focusing/defocussing mirrors, and are finally combined by a second wire grid polarizer in front of the CC waveguide aperture.

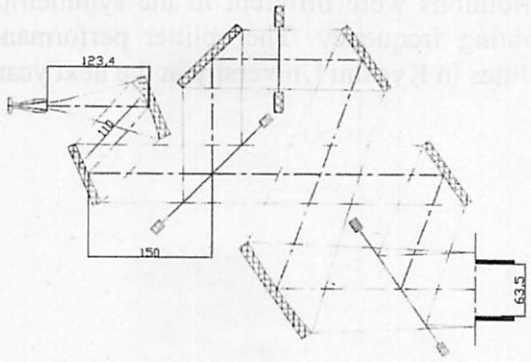

FIG.2: Schematic of the two Gaussian beam system. The system was composed of a corrugated horn antenna and quasi-optical mirrors, beam splitter/combiner.

The HE_{11} mode exciter using two Gaussian beams was tested at low power facilities. Figure 3 shows measured intensity and phase profiles at the waveguide entrance. A broader intensity profile was obtained, compared to the Gaussian beam as shown in a broken line. Especially, a flat phase profile was attained. The evaluated mode contents of the HE_{11} mode was 0.98.

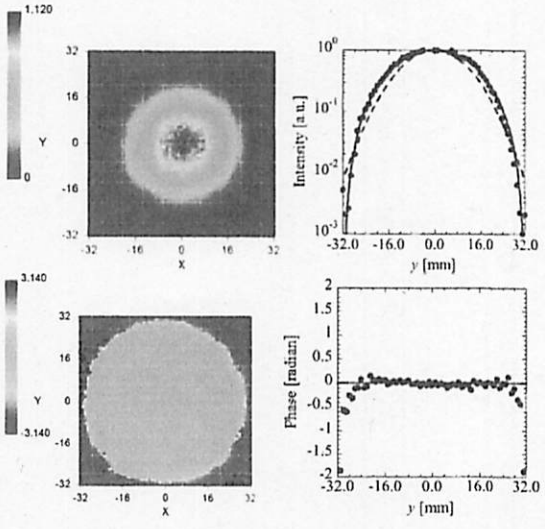

FIG.2: Measured intensity and phase profiles at the waveguide entrance of the HE_{11} mode exciter using two Gaussian beams.

Dual frequency FADIS

A FAst DIrectional Switch (FADIS) performance based on a steep slope in the diplexer transmission function was considered for dual-frequency (dual-*f*) applications. The switching between the output transmission lines is performed by frequency control of the source. A diplexer for a FADIS system using a Square Corrugated Waveguide (SCW) splitter was designed as one of the most attractive candidates for the dual-*f* operation.

The splitter performance is a key issue for the dual-*f* operation, and extended operation regions in splitter operations have been considered and surveyed using mode contents analysis based on matching coefficient evaluation. Some operational branches with high matching coefficients (> 0.9) were found, and new operating parameters were proposed for the dual-*f* operation in the JT-60SA ECHCD system. Radiation pattern distributions from the SCW splitter were defined very well with no serious side lobes in the dual-*f* operation. In the double-loop ring-resonator system, the diplexer frequency response was sufficiently steep to switch the outputs of the JT-60SA dual-*f* gyrotron. A bell-shaped corrugation profile is considered to reduce the Ohmic loss in the SCW and to construct the resonator ring at small phase difference in the dual-*f* application for arbitrary polarization states. The diffraction losses should be properly considered in real component-design because the two split beam distributions were different in the symmetric and anti-symmetric directions at the specific operating frequency. The splitter performance is going to be checked at the low-power facilities in Kyushu University in the next year.

国際化推進共同研究概要

No. 3

タイトル: Joint study of long pulse high beta discharges and related egde turbulence transport in steady state operation (SSO) plasmas on QUEST and EAST

研究代表者: GAO, Xiang

所内世話人: 花田 和明

実 施 期 間: 2014 年 12 月 3 日 ～ 12 月 10 日

研 究 概 要:

本年度は現在中国の ASIPP で稼働中の干渉計と製作中の偏光計の議論を実施した。また、本年度の QUEST 実験で得た Blob(ブロッブ)に関するデータの解析方法についての議論を行った。ガスパフが誘導する Blob の変化についての定量的議論を行うためのレート方程式の基本的な結果を用いて議論を行った。

RESEARCH REPORT

Date Dec. 11, 2014

Visiting scientists: (name) Xiang Gao

(position) Professor

(university / institute) Institute of Plasma Physics,
Chinese Academy of Sciences

(name) Yinxian Jie

(position) Professor

(university / institute) Institute of Plasma Physics,
Chinese Academy of Sciences

(name) Haiqing Liu

(position) Associate Professor

(university / institute) Institute of Plasma Physics,
Chinese Academy of Sciences

Host scientist: (name) Kazuaki Hanada

(position) Professor

(university / institute) Kyushu University

Research period: (from) Dec. 3, 2014 (to) Dec.10, 2014

Research subject: **Joint study of long pulse high beta discharge and related egde turbulence transport in steady state operation (SSO) plasmas on QUEST and EAST**

Introduction

Long pulse high beta dicharge is one of important missions for ITER and future fusion reactors. Comparative and joint study of long pulse high beta discharges on QUEST and EAST is one of most important things because the special feature of these two devices (QUEST, SSO with High beta; EAST, SSO with full superconducting coils). Exploitation and integration of diagnostic systems and physics issues in these two devices and compare the two-side result would give many fruitful results. In 2014, on QUEST, great progress has been achieved on SSO operation. EAST has also achieved significant progress towards long pulse and high performance plasmas recently. For long pulse high beta discharges, wall conditioning and edge turbulence control are the most important issues. In QUEST, hydrogen recycling during long duration discharges was investigated and new QUEST-wall model can reconstruct the particle flux dependence. The hot wall had already installed in the vaccum vessel as a control knob of fuel circulation. And the blob phenomena was studied to understand the particle flux on first wall driven by edge turbulence. In EAST, lithium powder injection system was developed for wall conditioning and ELM control on EAST. And the tungsten top divertor was installed to investigate the ITER-like mono-block divertor configuration.

Recently experimental progress in QUEST and EAST

In QUEST, hydrogen fluence on the wall has a significant impact to core plasma behavior. Progression from low (LR) to high recycling(HR) was observed in full non-inductive long duration discharges up to 12 minutes on QUEST, as shown in figure 1. And more, And more, 54kA plasma sustainment in low aspect ratio configuration by 28GHz injection was achieved. The plasma shaping was almost kept for 1.3s, as shown in figure 2. Higher current of 66kA was non-inductively obtained by slow ramp-up of vertical field also. Different configurations, limiter, IBNULL, divertor, have been achieved in the steady state operation. Simplified QUEST-wall model can reconstruct the particle flux dependence for 400s long pulse discharges. For future plan, QUEST will be performed

under hot wall to improve the controllability of Hydrogen recycling during long pulse plasma discharges (1000s). Detailed discussions with Prof. hanada allowed us to gather more information regarding the long pulse discharge activities and compared with the conditions on EAST.

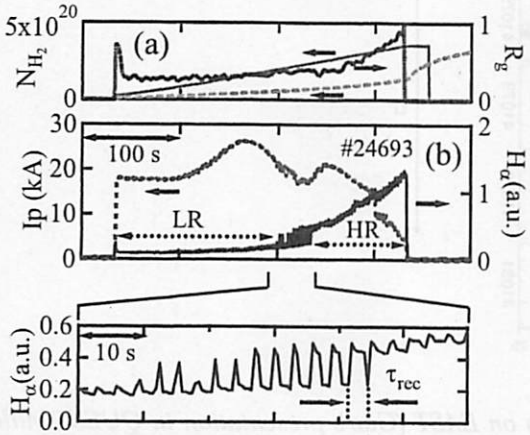

Figure 1 Hydrogen fluence on the wall has a significant impact to core plasma behavior (Prof. Hanada's presentation for discussions during this visit).

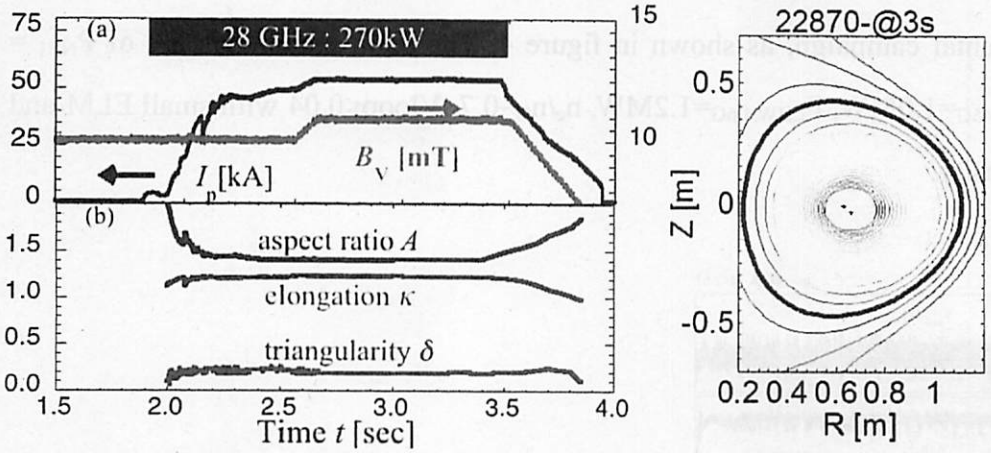

Figure 2 54 kA Plasma Sustainment in Low Aspect Ratio Configuration by 28GHz Injection (Prof. Hanada's presentation for discussions during this visit).

In 2014, EAST has some significant upgrades, including tungsten top divertor, cryopumps for both divertors, 10 MW LHCD+12MW ICRF + 4MW NBI, Resonant magnetic perturbation (RMP) coils, Polarimeter/interferometer(POINT) for current density profile etc. 18s ELM-free H-mode with Li injection was obtained, as shown in figure 3. In the ELMs H-mode discharges, the amplitude and frequency of ELMs are paced in a low level by Li

pellets successfully during H-mode. Heat flux level induced by paced ELMs is 50% lower compared with spontaneous ELMs.

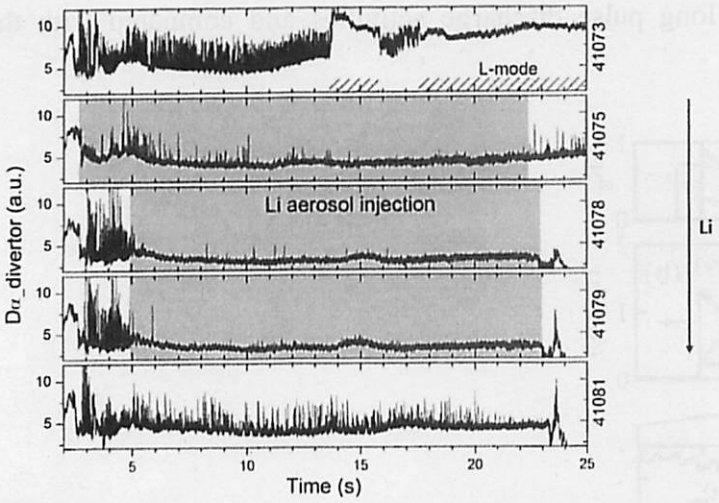

Figure 3 ELM-free H-mode up to 18s by Li injection on EAST (Gao's presentation in QUEST building during this visit).

Long pulse H-mode, > 20s, with LHCD+NBI modulation has been achieved in the 2014 EAST experimental campaign, as shown in figure 4. The main parameters are of P_{NBI} = 1.2MW, $P_{LHW,2.45G}$=1.0MW, $P_{LHW,4.6G}$=1.2MW, n_e/n_G~0.7, Vloop<0.04 with small ELM and controllable density.

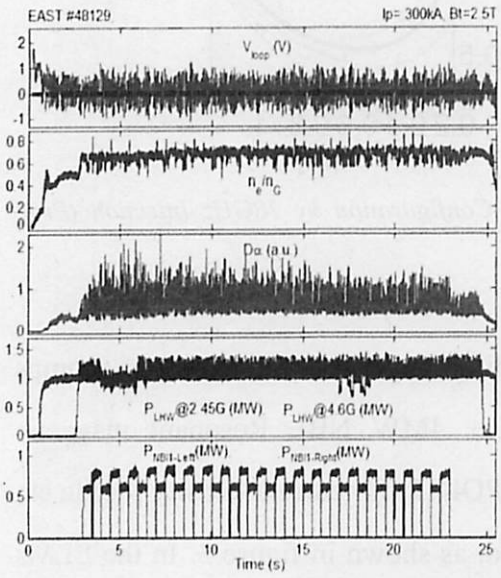

Figure 4 Long pulse H-mode with LHCD+NBI modulation (Gao's presentation in QUEST building during this visit).

Plasma activities associated with current density profile and electron density profile, the current density profile is key parameter for real-time plasma control (q profile and current density relaxation) for long-pulse discharges: connect plasma (diagnostics) – PCS - actuators (ICRH,LHCD) - plasma response and extend high-performance plasma regimes to long-pulse in preparation for ITER. The Polarimeter-interferometer(POINT) diagnostic has been installed on EAST for current profile measurement. Initial results of current profile from EFIT with Faraday rotation measurements was obtained, as shown in figure 5. The temporal resolution is up to 1us, the angle resolution ~ 0.1°, the the density resolution $1x10^{16}m^{-3}$. The POINT is the powerful tool for the real-time plasma control to get long pulse high beta discharges on EAST in future.

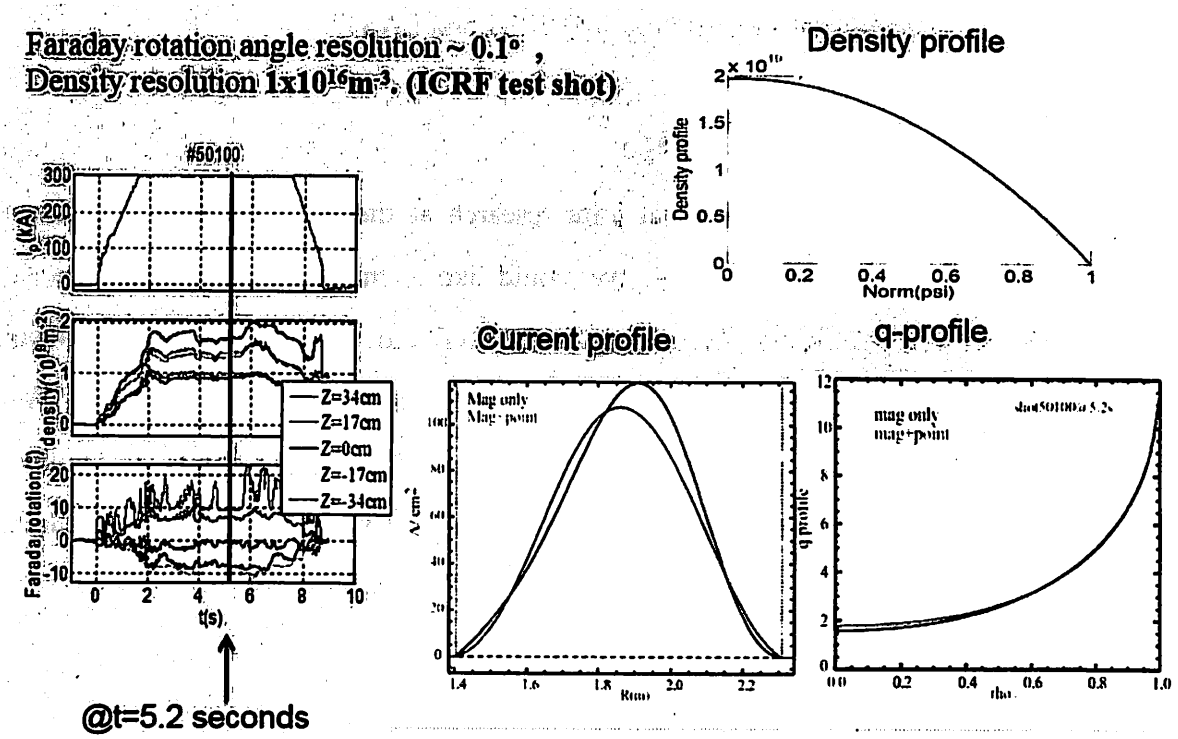

Figure 5 Initial results for current profile by POINT (Liu's presentation in QUEST building during this visit).

Discussions

QUEST and EAST are both to develop the scientific basis for achieving a steady state condition. Now here has a new start point for the comparative and joint study on QUEST and EAST, especially in long pulse high beta discharges, high performance SSO operation

for ITER scenario. QUEST has installed the ITER like hot wall. EAST has installed the ITER like tungsten top divertor and has 26MW heating power totally. The joint study results now and in future may shed light on the ITER SSO senario.

During this visit, several interesting topics are also involved in discussions. Those are "Non-inductive plasma current start-up using fundamental and second harmonic ECRH on QUEST" by Mr. Miura, "Calorimetric Measurement of Direct Loss of Energetic Electrons with Movable Limiters in Non-Inductive Current Driven Limiter Plasma with a microwave of 8.2 GHz on QUEST" by Mr. Hamada, "Enhancement of electron density and density skewness in blobs induced by fuel gas puffing in ECR plasmas on QUEST" by Mr. Oyama. Base on the detailed discussions on these topics, the decisions were done of QUEST students enjoy in the collaborative activities of QUEST and EAST.

Acknowledgement and comments:

Work supported by the international joint research at the Joint Usage of Research Centers for Applied Mechanics for 2014. We would like to thank our host, Professor K. Hanada, who helps a lot during my staying at QUEST and very appreciate the useful discussions and comments. It is a good chance for us to join in study in the QUEST. We hope that the international joint research at the Joint Usage of Research Centers for Applied Mechanics could continue to enhance China-Japan cooperation on fusion plasma research in the future.

(Signature)_____

(Name in print) Xiang Gao, Yinxian Jie, Haiqing Liu

国際化推進共同研究概要

No. 4

タイトル: Develop and improve EFIT code of tha plasma equilibrium reconstruction for SSO operation and advanced physical study on QUEST

研究代表者: QIAN, jinping

所内世話人: 花田 和明

実 施 期 間: 2014 年 12 月 3 日 ～ 12 月 10 日

研究概要:

本年度は国際標準的平衡コード EFIT によるプラズマ解析と実験データの比較を行った。計算された磁気面から粒子の軌道を計算し、可動プローブによる実験結果と比較することで大半径外側での磁気面の精度の確認ができることがわかった。実際の比較は今後行う予定である。27 年3月に九大の学生が1名、ASIPP を訪問し議論を進めている。

(様式 11・拠点)

RESEARCH REPORT

Date Dec. 11 2014

Visiting scientist: (name) Jinping Qian

(position) Associate Professor

(university / institute) Institute of Plasma Physics,
Chinese Academy of Sciences

Host scientist: (name) K. Hanada

(position) Professor

(university / institute) Kyushu University

Research period: (from) Dec. 3, 2014 (to) Dec. 10, 2014

Research subject: **Develop and improve EFIT code of the plasma equilibrium reconstruction for SSO operation and advanced physical study on QUEST**

The mission started on Thurday 4th December 2014, when our host, Professor K. Hanada, welcomed us on site and led us to the meeting room. Afterwards, Professor Hanada introduced the recent progress and future plan on QUEST in 2014. During the presentation, attention was given to low and high hydrogen recycling during long duration discharges, where hydrogen fluence on the wall has a significant impact to core plasma behavior. And more, limiter, IBNULL, divertor has been achieved in the steady state operation. For future plan, QUEST will be performed under hot wall to improve the controllability of wall-pumping, especially the Hydrogen. Discussions with Hanada sensei allowed us to gather more information regarding the long pulse discharge activities, which will allow us to better estimate the conditioning of EAST.

Three students gave their research presentations submitted to the A3 meeting. During the presentations, Miura showed us the non-inductive plasma current start-up using O-mode fundamental (1st) and second harmonic(2nd)electron cyclotron resonance heating (ECRH) of 8.2GHz, where the vacuum vessel temperature was kept ~370K, and there was no null field inside the main chamber for the breakdown. This non-inductive, hot wall operation will be benefit for future EAST research towards the steady state high performance. Meanwhile, this non-inductive plasma current start up can also contribute to those superconducting tokamak, like EAST, with the limitation of poloidal field current variation. Then Hamada introduced the head load in the Movable Limiters for non-inductive current drive with a microwave of 8.2 GHz on QUEST, where the main head load was contributed by electron.

During our stay, professor Gao and Liu gave two presentations, one is recent EAST progress and another is EAST POINT diagnostic system. More discussions about further cooperation between EAST and QUEST were hot up. Several students of QUEST will visit ASIPP soon in the coming financial year.

Miura and I discussed the EAST start-up, including the poloidal field coil initialization, null field, breakdown, program control, RZIP feedback, iso-flux control. This could be the warm up for his ASIPP visit, the ohmic start-up on EAST.

During our visit, QUEST did not start the experiment of this campaign, Hamada and I talked the EFIT reconstruction for the QUEST long pulse data based on the last campaign. As usual, EFIT could be run automatically when all magnetic data was uploaded in the Linux PC (see report Feb, 2014). In addition, our collaboration of EFIT paper algorithm validation of the current profile reconstruction based on Polarimeter/Interferometer (POINT) was accepted and will be published Plasma Science and Technology, Vol.17, No.1, Jan. 2015.

As a conclusion to this visit, we of the EAST experiment team warmly thank professor Hanada for welcoming us and showing us QUEST activities and very appreciate the useful discussion and comments between EAST and QUEST.

(Signature) J. Qian

(Name in print) Jinping Qian

国際化推進共同研究概要

No. 5

タイトル: RF-only ST plasma confinement, sustainment, and interactions with wall materials

研究代表者: PENG, Yueng-Kay, Martin

所内世話人: 花田 和明

実 施 期 間: 2015 年 3 月 25 日 ～ 3 月 26 日

研 究 概 要:

平成２７年３月２５－２６日の２日間に国際 WS を開催した。欧州から２名、TV 会議システムで米国から２名、国内の学外者が４名と応研関係者の参加があった。今回は MAST の Shevchenko 氏の共同研究との共催として実施した。残念ながら Peng 氏は参加できなかったが、第１回、第２回ともにワークショップに参加した Shevchenko 氏が中心となって QUEST の電子バーンシュタイン波加熱・電流駆動及びプラズマ・壁相互作用に関する議論を実施した。議論の内容は 26 日に Shevchenko 氏によってまとめられた。

Third Kyushu Workshop on Solenoid-Free RF-Only ST Plasmas

March 25-26, 2015

A program of the Workshop is the followings.

25-March AM
9:30-
Vladimir Shevchenko / Kazuaki Hanada
WS purpose and agenda
9:40-10:40
Mikhail Gryaznevich
Overview of ST40 project
10:40-11:25
Vladimir Shevchenko
Analysis of EBW start-up experiments and EBE measurements on MAST

PM (RF-only Plasma Start-up and Equilibrium)
12:45-13:30
Yuichi Takase
Recent progress in the TST-2 RF start-up experiments (tentative)
13:30-14:15
Akio Ishida
Three-fluid equilibrium considerations of a RF-sustained ST plasma (tentative)
14:15-15:00
Hitoshi Tanaka
Observation and analysis of vertical and toroidal currents in toroidal ECR plasmas in the LATE device

Coffee Break

15:10-15:30
Akira Ejiri
Ion temperature and flow measurements on TST-2 and LATE
15:30-16:15
Kishore Mishra
Intrinsic rotation in QUEST Plasma: From open magnetic field configuration to steady state high betap IPN plasma
16:15-17:00
Hiroshi Idei
Dual frequency (8.2 / 28 GHz) Electron Cyclotron Heating and Current Drive Experiments in QUEST

26-March
AM (RF-only Plasma Sustainment and PWI)
9:00-9:45
Alexander Kuzmin / Hideki Zushi
Plasma Permeation Diagnostics / Plasma response function for long pulse operational parameters in QUEST (tentative)

9:45-10:30
Kazuaki Hanada
Investigation of particle balance in long duration discharges on QUEST

10:30- All Suggested focus and output for this joint drafting session
10:45- Yuichi Takase
RF-only ST and large tori plasma properties
10:45- Vladimir Shevchenko
RF technology, plasma diagnosics
10:45- Kazuaki Hanada
Heat and particle handling
12:15- Vladimir Shevchenko
Summary

In the section devoted to RF-only plasma performance and equilibrium five talks have been presented and discussed.

By Prof. M. Gryaznevich from Tokamak Energy Ltd, United Kingdom

Recent advances in the development of high temperature superconductors (HTS) [1], and encouraging recent results on a strong favourable dependence of electron transport on higher toroidal field (TF) in Spherical Tokamaks (ST) [2], open new prospects for a high field ST as a compact fusion reactor or a powerful neutron source. The combination of the high β (ratio of the plasma pressure to magnetic pressure), which has been achieved in STs, and the high TF that can be produced by HTS TF magnets opens a path to lower-volume fusion devices, in accordance with the fusion power scaling proportional to $\beta^2 B_t^4 V$. A compact ST is also a promising candidate for an intense and efficient neutron source [3].

Overview of the ST40 project was presented. Main objectives of the project, parameters of the tokamak, physics programme issues are described and physics and engineering challenges of this device are discussed. The present status of the construction is reported. Discussions of physics issues include plasma formation using merging-compression, results of transport simulations of OH and auxiliary heating regimes and detailed predictions for the expected plasma parameters, results of the plasma vertical stability simulations and optimization of passive plates position, divertor design and power loads, some aspects of fast particle physics. Results of optimization of the neutral beam current drive are presented in detail.

Recent progress on small tokamaks ST25 and HTS-ST is also overviewed. ST25 is a small tokamak (R/a=25/12.5cm, B_t=0.1-0.3T) with Cu magnets and long pulses up to 28 seconds have been recently produced using 2.45 GHz RF power. Results of EBW current drive experiments using both high field side and low field side launch are presented. The HTS-ST is a similar size tokamak but with all-HTS YBCO magnets cooled down to 20-30K and 24h operations have been recently performed.

The demonstration of reliable steady state operations in a compact ST even at the level of a few MW Fusion output as a first step will significantly advance not only the mainstream Fusion for the Energy research, but also the commercial exploitation of Fusion and will the an important step on development of the Fusion Energy.

[1] M GRYAZNEVICH et al., "Progress in applications of High Temperature Superconductor in Tokamak Magnets". *Fusion Eng. and Design*, **88** (2013) 1593–1596.

[2] M. VALOVIC et al., *Nuclear Fusion*, **49** 075016 (2009).

[3] M GRYAZNEVICH et al, "Options for a Steady-State Compact Fusion Neutron Source". *Fusion Science and Technology* **61** 1T 89 (2012)

By Prof. Y. Takase from University of Tokyo

Plasma start-up and plasma current ramp-up using the lower hybrid wave (LHW) at 200 MHz are being studied on TST-2. Three different types of antennas have been used: the inductively-coupled combline (ICC) antenna, the dielectric-loaded waveguide array (grill) antenna, and the capacitively-coupled combline (CCC) antenna. The ICC antenna excites the fast wave (FW), and requires mode conversion to the LHW for efficient current drive. The grill antenna has high overall reflectivity and the reflectivities of the four waveguides of the array are unbalanced, resulting in deterioration of the $n_{//}$ spectrum of the launched LHW. The CCC antenna can excite the LHW with good $n_{//}$ spectrum, in principle. However, in the present configuration, antenna-plasma coupling is too strong, and the excited $n_{//}$ spectrum is not optimum. Based on wave excitation modeling using COMSOL (commercial finite element code), improvements are suggested to reduce antenna-plasma coupling and to reduce reflection from the antenna protection limiter.

The dependences of the current drive efficiency and hard X-ray energy spectrum on the excited spectrum were studied by changing the phasing between adjacent waveguides of the grill antenna. It was found that low $n_{//}$ favors acceleration of electrons to higher energies and higher current drive efficiency. The wavenumbers of the excited LHW and FW measured by a magnetic probe array were found to be lower than that excited by the antenna.

The current drive efficiency was found to be the highest for the CCC antenna and the lowest for the ICC antenna. In all cases the driven current increases with the vertical field, and with the toroidal field. Hard X-ray measurements indicate higher co/ctr ratio for the CCC antenna compared to the grill antenna, and a broader spatial profile for higher energy X-rays. The X-ray intensity is higher and the spatial profile is more centrally peaked at higher toroidal fields. A density limit was observed around line average electron density of 0.5×10^{18} m^{-3}. This does not seem to be caused by parametric decay. Although accessibility does degrade wave penetration at higher densities, the observed abrupt limit is not predicted. The cause of this limit is under investigation.

In order to reduce the effect of edge losses which may be responsible for degradation of current drive, a top-launch antenna is being designed in collaboration with C. Moeller of GA. In order to extend the operational regime to higher toroidal field (up to 0.3 T) for longer durations (100 ms), an upgrade of the TF and PF capacitor banks is planned.

By Prof. A. Ishida

Three-fluid equilibrium considerations of a RF-sustained ST plasma*

*This work was done in collaboration with Akira Ejiri (University of Tokyo) and the TST-2 group

After the 2nd Kyushu workshop held in February 2014, we recognized importance of energetic electrons. Since then, we have developed three-fluid equilibrium model which consists of the ion fluid, the el-electron fluid and the eh-electron fluid. Here we assume the charge neutrality, $n_i=n_{el}+n_{eh}$, $n_i >> n_{eh}$, and $T_i<T_{el}<<T_{eh}$. In this workshop we presented formalism of the three-fluid axisymmetric equilibrium model in comparison with the familiar GS model to show similarity and differences between the two. Then we applied the three-fluid model to the recent TST-2 experiment of #115620 at 80ms. To solve the partial differential equation for the magnetic flux, we used the flux data of the above shot on the computational boundary. We showed one example of the reconstructed equilibrium which satisfies the toroidal current densities at the inboard and outboard limiters are zero. This equilibrium also realizes some target data of the experiment such as the plasma current, the electron density, the electron and ion temperatures and small ion toroidal velocity. In this comparison, it is found that the three-fluid equilibrium model is useful and flexible although it is somewhat complex. We like to improve the model by comparing more detailed profile with experiments

By Prof. H. Tanaka from Kyoto University

Observation and analysis of vertical and toroidal currents in toroidal ECR plasmas in the LATE device

Observation on conversion from vertical charge separation current to the toroidal current has been made for the first time in toroidal ECR plasmas in the LATE device. Both the vertical and toroidal current are sort of equilibrium current to balance radial ballooning force by the counterforce of $j_z\hat{z} \times B_\phi\hat{\phi}$ and $j_\phi\hat{\phi} \times B_z\hat{z}$, respectively. The latter toroidal current brings about a closed flux surface when it develops large enough to generate so-called cross field passing electrons.

Experimental results and analyses using fluid model show that while the former counterforce dominates over the latter when Bv is very weak, the toroidal current increases and the latter counterforce becomes dominant with Bv and finally a closed flux surface is generated when a sufficient microwave power is injected. In the case of a discharge with a steady Bv, while the former counterforce is initially dominant because toroidal current is very low in early stage, the latter counter force from the toroidal current eventually becomes dominant and finally a closed flux surface appears.

By Prof. H. Idei from Kyushu University

Collaboration among National Institute for Fusion Science, Tsukuba Univ. and Kyushu Univ. has been begun since 2011. 28 GHz Electron Cyclotron Current Drive effect was clearly observed in ohmically heated plasmas with feedback regulation of Center Solenoid coil current in 2nd harmonic inboard off-axis heating scenario. In non-inductive current drive experiments only by the 28 GHz injection, 54 kA plasma current was sustained for 0.9 sec. High non-inductive plasma current of 66 kA was also attained by the 28 GHz ECH/ECCD. The plasma equilibrium of the 28 GHz start-up plasma was analyzed. A large volumed plasma equilibrium was evaluated in the analysis. The last closed flux surface (LCFS) boundary was at R=1.15 m where is beyond the 2nd harmonic resonance position of

8.2 GHz injection. Spontaneous density jump across 8.2 GHz cutoff density was observed in simultaneous 28 GHz / 8.2 GHz injections. Using the density jump phenomena, the high density plasma of the 25 kA level was obtained in the simultaneous injection. In the simultaneous injection, the LCFS boundary was not beyond the 2nd harmonic resonance position of 8.2 GHz injection. The electron pressure required for the equilibrium was much higher than the bulk electron pressure measured by Thomson scattering diagnostics, indicating fast electron pressure carrying the plasma current was dominant in the plasma. Larger energetic HX intensity was observed in the 8.2 GHz interaction region, compared to the 28 GHz interaction region. The electron temperature Te was high near the off-axis positioned 28 GHz 2nd harmonic resonance layer, while Te was significantly high near the fundamental 8.2 GHz resonance in the low density phase also. In the high density phase after the spontaneous density jumps, Te was started to be increased in the core region. This Te increment was not explained by the 28 GHz interaction because Te was already decreased even in the 28 GHz resonance layer in the high density phase. Some heating effects were observed in over dense core region by the 8.2 GHz injection. The parallel refractive index required to explain the heating effect by the EBW interaction was evaluated to be 4. If the 8.2 GHz power was superposed to the 28 GHz large volume target plasma, the plasma current was so decreased into the 10 kA level. The magnetic axis was moved outside once, and inside later. Large magnetic axis was observed due to the large Shafranov shift by the fast energetic pressure in the 8.2 GHz 2nd harmonic interaction outside, and then plasma was shrunk into the omelette shaping with small ellipticity. If the Bv was added in the 8.2 GHz superposed phase to move the plasma inside avoiding the 8.2 GHz interaction outside, the 50 kA plasmas were sustained by the superposed 8.2 GHz injection to the 28 GHz target plasma in the stable plasma shaping.

In the section devoted to RF technology and plasma diagnostics five talks and one proposal have been presented and discussed.

By Dr. V. Shevchenko from Culham Centre for Fusion Energy, United Kingdom

Summary from MAST

Strong microwave bursts with intensity more than a factor of 1000 greater than thermal emission have been seen on MAST during Edge Localised Modes (ELM) events. High time resolution measurements reveal each ELM burst to be composed of many shorter ~1μs events clustered together. Synthetic Aperture Microwave Imaging (SAMI) shows these bursts to be highly spatially localised and to originate preferentially from the midplane region. Non-ideal MHD fluid simulations of ELMs in MAST show that parallel electric fields of 2 kV is present on the boundary during ELMs. These fields generate a population of fast electrons at the plasma boundary. As confirmed by PIC modelling bursting emission comes from fast electrons via the collective anomalous Doppler instability.

Simultaneously with 'passive' thermal emission imaging SAMI operates in the 'active' probing mode. Measured backscattered spectra are complicated. Signals generated by different effects can be filtered out and analysed separately. Signals with small Doppler shifts can be used to form images providing flow directions. Coherent modes are usually visible by other diagnostics as well. Their data

must be analysed together. Signals with large Doppler shifts must be analysed separately. Image reconstruction is not developed yet for this case.

Strong ECE in start-up experiments was observed around fundamental ECR during plasma current ramp-up. These ECE bursts are about 2 orders of magnitude stronger than thermal ECE. A Cyclotron Maser Instability (CMI) is considered as a potential explanation for these bursts. CMI is easily developed in plasmas with $\omega_{pe}/\omega_{ce} << 1$ which is typical for EBW start-up. Modelling based on a ring-beam distribution (RBD) predicts that two types of CMI are relevant for EBW start-up plasma: Z1 for the RBD angles 75-90 degrees and Beam-Whistler (B-W) for the angles below 75 degrees. Z1 and B-W modes develop opposite signs of $k_{||}$ so they transfer momentum to the electrons in opposite directions. Z1 (S-X) or B-W CMI (co- or counter-CD) will dominate depending on the velocity pitch angle in the RBD. CMI current drive does not require electron collisions. CMI can explain both the current ramp and ECE bursts correlated with this ramp.

Proposal: *It would be interesting where possible to measure fundamental ECE from in other start-up experiments using LH CD (TST-2), QUEST (X2 ECRH), LATE etc.*

Is this the ECE burst effect during current ramp-up unique for MAST?

By Prof. H. Idei from Kyushu University

In 28 GHz system on QUEST, simplest transmission and launcher system have been prepared to conduct the high density discharge for the 8.2 GHz EBW experiments. Polarizer system was not prepared for a 2nd harmonic resonance scenario, and O-mode wave was injected into the plasma without focusing launcher-mirror system. In order to conduct the local ECH/ECCD experiments, large focusing mirror system is designing for the 28 GHz injection. A focusing beam with a 5cm waist size will be injected with X-mode polarization control in both of perpendicular and oblique (also tangential) injections. This large focusing mirror will have a different focusing curved surface in a behind face to conduct the 8.56 GHz experiments. The 8.56 GHz power will be launched from rectangular waveguides in two orthogonal wave-electric fields, and will be focused with the large mirror. The radiation fields from the waveguides were evaluated by a developed Kirchoff integral code, and the mirror surface was designed from the phase distribution of the beam radiated from the waveguides.

By Prof. A. Ejiri

Ion flow and ion temperature were measured spectroscopically using the CIII line (C^{2+}, 464.7 nm) in TST-2 and LATE in RF (LH in TST-2, EC in LATE) sustained plasmas with I_p = 8-9 kA. In TST-2, $T_i \sim 5$ eV, toroidal flow is ~ 1 km/s, poloidal flow is < 1 km/s, and $|E_r| < 50$ V/m. In LATE, $T_i \sim 10$ eV, toroidal flow is ~ 5 km/s, poloidal flow is ~ 5 km/s, and $E_r \sim +300$ V/m. The flow velocities are small and the centrifugal forces can be neglected in the force balance. These electric fields are not as large as those expected based on fast electron losses alone. Although the ion temperatures are low (5-10 eV), ion orbit losses can be significant due to the large orbit deviation from flux surfaces.

By Dr. K. Mishra from Kyushu University

Plasma rotation (both toroidal and poloidal) has a key role in the regulation of instabilities, L-H transition, suppression of turbulence, improvement in energy confinement time etc [1]. Externally

torque induced plasma rotation has been studied with auxiliary inputs like NBI, ICRH, IBW etc. However, in large devices and fusion machines, intrinsic rotation generated within the plasma has more perspective. Intrinsic rotation in plasma has been triggered in many tokamaks with application of ECRH, RMP driven modification of NTV among others. Many explanations including equilibrium poloidal E x B flow, the sheath physics, and the presence of poloidal asymmetries in the pressure profile acting as sources of momentum have been given [2]. Even some most favorite explanations of simple increase in momentum diffusivity, modification to the external torque deposition profile, a preferential loss of fast ions from the plasma core, or an interaction of core modes with the vessel wall cannot explain intrinsic rotation observed at times [3]. In short, origin and controls of plasma intrinsic rotations have not been fully understood till date.

To understand intrinsic rotations in tokamak plasma, simple torus plasma rotation has been investigated in TORPEX device in past [4]. Although the rotation is believed to be influenced by motion of density blobs, its origin could not be identified fully. In QUEST device, such intrinsic rotation in simple ECR slab annular plasma with open magnetic field configuration is being investigated. It is observed that, toroidal rotation originates from the ECR layer in the vicinity of sharp density gradient region. Rotation amplitude and profile are found to be controlled by the choice of applied magnetic mirror ratio, vertical field strength and resonance location. The rotation in this open field line is evolved to co-current rotation in fully formed steady state high β_p Inboard Poloidal magnetic field Null (IPN) plasma in closed magnetic field configuration. However, it is observed that this rotation is dependent on equilibrium configuration, strength of the vertical magnetic field and its mirror ratio. While toroidal rotation velocity up to 20 km/s is observed in IPN configuration, negligible rotation is seen in case inboard limiter plasma.

The proposed future work to investigate the rotation consists of followings.

1. Developing a fast and reliable model to invert the observed integrated measurements to local profiles.

2. To compute, estimate and identify various sources of rotation like E x B_θ, E x B_ϕ , ∇B drift, ∇p etc.

3. Investigating similar rotation in open magnetic field configurations in other ST devices like TST-2, LATE etc. to complement the ongoing detailed investigations of rotation on these machines.

[1] R. J. Goldston, Nucl. Fusion **52**, 013009 (2012) and references therein.

[2] J. Loizu et al, PHYSICS OF PLASMAS 21, 062309 (2014)

[3] R M McDermott, et al, Plasma Phys. Control. Fusion 53 (2011) 035007

[4] B. Labit et al., PHYSICS OF PLASMAS 18, 032308 2011

By Dr. A. Kuzmin from Kyushu University

Hydrogen (H) retention in long duration steady state tokamak operation (SSTO) is studied in QUEST spherical tokamak using . H plasma was started-up non-inductively with RF [1,2] systems; Typical parameters in the core and SOL/wall regions for SSTO driven by electron cyclotron waves ECWs are as follows: T_e~ 400-600 eV, nl ~ 1-2×10^{18} m^{-2}, T_i is 10-20 eV. The magnetic field B_T is 0.15 T and I_p is 20 kA. In the SOL and on the top and bottom plates, T_e^{sol} ~ 5-20 eV, n_e^{sol}~2-6×10^{15} m^{-3}, and T_e^{div} ~ 5-10 eV, measured by Langmuir probe arrays. The RF power at 8.2 GHz is < 100 kW. The vacuum vessel consists of fully metallic (SS and W) plasma facing materials (PFM), vessel radius and height are 1.4 m and 2.8 m, respectively.

Usage of all metal PFMs allows to reduce the long-term retention rate of H isotopes by factor of 10 – 20 compared with carbon PFMs [3]. In QUEST during SSTO net wall retention, estimated with global gas balance, was ~ 70 – 80% of the fuelled H amount. To prolong SSTO duration gas injection should be reduced when PFM are saturated with H and neutral pressure is mainly determined by the H release from PFMs. With feedback control of gas injection to keep H_α radiation in a given range it was possible to maintain SSTO for ~820 sec. In the second half of discharge no gas was fuelled, reducing possibility for discharge control.

PdCu membrane probes are used in QUEST tokamak for hydrogen retention flux measurements at several position. Incident flux could be calculated solving diffusion equation and fitting experimental permeation curve varying unknown parameters: recombination coefficients. Coefficients calculated from fit procedure are in agreement with laboratory results for the same PdCu alloy. Distribution of the retention fluxes in long steady state tokamak operation shows high importance of atomic hydrogen irradiation of the SS walls far from the main PWI areas.

[1] H. Zushi et al., 21st IAEA FEC (2012)

[2] H. Idei et al., 21st IAEA FEC (2012)

By Dr J. Caughman and Dr T. Bigelow from ORNL, USA

An area of interest for us is microwave coupling to the plasma for both startup and non-inductive current drive. Have you considered a high-field launcher configuration for the 8.2 GHz injection? We would also be interested in investigating a steerable mirror configuration for low-field 28 GHz launch, too. We would be interested in collaborating in these areas, as well as potentially participating in experiments. The combination of CHI and ECH/EBW is another area of interest for us.

In the section devoted to the Heat and particle handling two talks have been presented and discussed.

By Prof. K. Hanada from Kyushu University

Investigation of particle balance in long duration discharge on QUEST

The mission of QUEST is survey at the time of finishing Phase II.

"In Phase II (6 years:2010-2015) , progress towards higher current (~100 kA) in steady-state, and towards higher beta (~10%) in the pulsed operation will be pursued with an upgraded heating system."

The scientific base for plasma current of 100kA could be obtained with 28GHz 1MW, CW, which is developing in the collaborating work with Thukuba University. To achieve higher beta, additional heating sources such as NBI are required, however it is still difficult.

In the view of steady state operation, the power handling was done with two water-cooling W block limiters on the outside vessel and eight water-cooling W blocks located on the divertor plate. Almost 50% of the injected power deposited on the vacuum vessel and it mainly comes from leak RF power. The improvement of RF absorption is still problem. The result of improved power handling gives the longest discharge up to 810s using 8.2GHz RF and particle handling is the next issue.

The particle handling, especially fuel recycling is a crucial issue to get better confinement core plasma. In JET, dynamic retention is dominant in ITER-like wall experiments and long duration discharge in QUEST in the same. Investigation of the model is established and could explain the behavior of hydrogen recycling in the long duration discharges on QUEST. The model indicates that the control of surface recombination rate of the metal wall using wall temperature can modify the recycling rate. QUEST has a plan to control the wall temperature with the hot wall and further development is expected.

By Prof. H. Zushi from Kyushu University

The global gas balance in the various types of steady discharges has been re-examined by measuring the partial pressures of hydrogen and helium, and plasma induced permeated flux at various positions. A new approach to study the dynamics of particle circulation in steady state tokamak operation SSTO has been proposed and demonstrated in QUEST with all metal walls baked at 100°C. Using perturbations of particle source H_2 and plasma-wall interaction PWI the system functions of processes of retention and release into/from the wall are determined both in time and frequency domains. The time dependent probability function of the transition between high and low recycling states has been derived.

In summary, the global gas balance is examined in QUEST from a view point of how the retention ratio R deviates from the ideal zero value in various types of discharges. Since this global gas balance method has an intrinsic disadvantage for identifying the retention and release processes, additional diagnostics for them have been introduced. Using the PDP signals and the TMAP7 code, the retention fluxes can be deduced at various positions and it is found that the reduction in the retention flux contributes to the small change in R. The local maximum of R with respect to the amount of the fuelled H_2 is also investigated by independent measurement of the retention flux and released one. The new technique to understand the dynamics of the particle circulation in the system has been introduced and demonstrated for the various kinds of perturbations. The system response functions can be obtained in time and frequency domains and advantages of this method have been shown for the quantitative fraction of the retention and release components induced by the local and temporal perturbations. In SSTO it is noted that the recycling feature caused by retention and release processes evolves in the discharge duration. The time dependent probability function for the resident time for HR is derived, which can describe how the particle circulation

process develops during the discharge. To understand mechanisms dominating time dependent feature of the probability function will be the next step along the present study.

国際化推進共同研究概要

No. 6

タイトル：CHI experiment and the related research on plasma physics in QUEST

研究代表者：NELSON, Brian, A

所内世話人： 花田 和明

来訪期間 ： 2015 年 1 月 18 日 ～ 1 月 24 日

概要：

本年度は、ダイバータ板を 15cm 降下させる作業とCHIの電極設置を行った関係で、CHIに関する実験は実施できなかった。そのため米国予算で作成している電源設備に関する検討を実施した。電源の基本的性能や運転シーケンス、安全対策を確認し、九州大学で作成した光絶縁信号の送受信の試験を実施した。この結果は米国製の電源の製造に反映されて6月の実験開始に向けた最終チェックが完了した。

Proposal for the Operation of CHI on QUEST *
24 February 2015

R. Raman[1], T.R. Jarboe[1], M. Ono[2], K. Hanada[3], B.A. Nelson[1], M. Nagata[4]
[1] University of Washington, Seattle, WA, USA
[2] Princeton Plasma Physics Laboratory, Princeton, NJ, USA
[3] Kyushu University, Kyushu, Japan
[4] University of Hyogo, Himeji, Japan

This proposal is for a US-Japan collaborative research between Kyushu University and the University of Washington for completing the implementation of Coaxial Helicity Injection (CHI) capability in the QUEST Spherical Torus at Kyushu University, and to begin operating the system to generate Transient CHI discharges. This report is an update to the previous report dated 28 March 2014. Therefore, information from the previous report is only mentioned briefly, so as to make this report easier to read.

On QUEST, CHI is capable of contributing towards multiple roles. These include: (1) Solenoid-free plasma start-up: CHI can generate significant amounts of non-inductively generated closed flux plasma current through the process of *transient* CHI. (2) Edge biasing: By driving few kA of current along the outer scrape-off-layer (SOL), it provides a means to inject density along the SOL and thereby increase the edge density and vary the density gradient near the separatrix region in support of EBW current drive studies. (3) Steady-state current drive: By continuously driving current along the scrape-off-layer, it offers the possibility of continuous current drive to modify the edge current profile. The all-metal nature of QUEST in addition to its capability for 400 kW of ECH power would both reduce the amount of low-Z impurities initially injected during the application of CHI and because of its ECH heating capability allow a relatively greater fraction of the injected low-Z impurities to burn through radiation barriers, which is necessary for generating a discharge with good confinement.

Brief summary of activities during the past year:

During the period of March to June 2014, the CHI design was finalized. An important change to the design was an improved design for the current feed. Figure 1 shows the new design. The design eliminated ceramic vacuum current feedthroughs, because they have the potential to fracture when subjected to J X B forces during operation. The new design used a custom vacuum feedthrough that relies on about a 2 cm diameter stainless steel rod and a O-ring based Peek insulator for achieving the required insulation, while providing sufficient flexing ability to the system. The O-ring seals are located outside the vessel structure, where the ambient temperatures are low.

The University of Washington procured the required ceramic tiles from Kyocera Corporation, and delivered it to Kyushu University. A photograph of the sixteen insulator segments, assembled to form a continuous ring, is shown in Figure 2.

---

* We acknowledge helpful discussions with Prof. Zushi, Mr. Noda (V-Tech Limited) and Mr. Rogers (Univ. of Washington) and with other members of the QUEST Team.

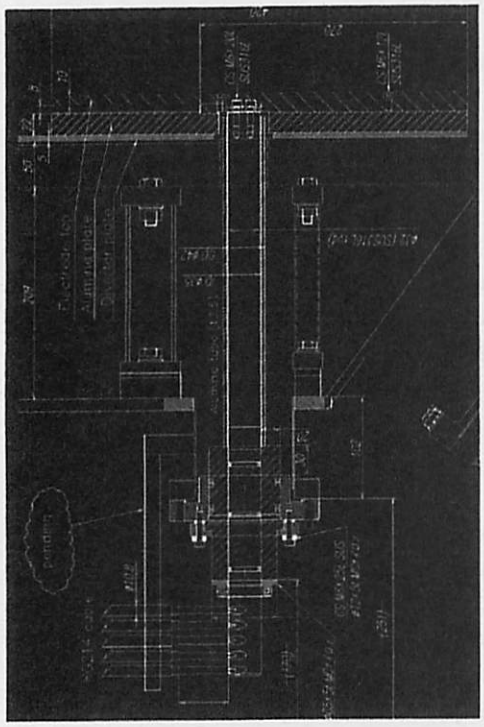

Figure 1: Current feed design for CHI. The plate with the yellow hatches inclined the right is the insulator plate. The top most plate with the hatches inclined to the left is the electrode plate. The current feedthrough is located at the bottom of the long rod.

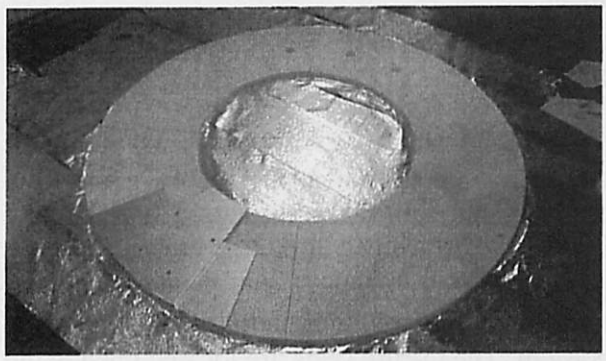

Figure 2: CHI insulator required for achieving voltage isolation between the electrodes and the vessel.

These have now been installed in QUEST. Figure 3 shows the final electrode installation on QUEST that shows the top of the electrode plates that are positioned on top of the ceramic plates, as shown in the Figure 1 view.

The capacitor bank necessary for CHI operations is being built at the University of Washington and will be shipped to Kyushu University later this year. Figure 4 is a layout of the capacitor bank components. The University of Washington will also provide a capacitor-based snubber system that will be connected to the bottom of the current feed rod, at the same location where the current feed cables from the capacitor bank connect to the current feed rod. It will also provide the gas injection system.

The details of the capacitor bank operation logic, and CHI gas injection system logic were finalized during January 2015. The additional hardware changes requested by QUEST personnel are being incorporated into the capacitor bank system. The capacitor bank and the gas system will be operated remotely from the QUEST Control Room using LabView based control software that will be written by QUEST personnel. The software interacts with the primary QUEST control system so that information related to the capacitor bank and gas system's readiness for CHI operations could be recognized by the main QUEST control system, which will then provide the needed signals to trigger these systems. The capacitor bank produced current, which is the CHI injector current, and the capacitor bank charging voltage will be archived within the QUEST database. Fast voltage measurements at each of the current feed locations will also be measured. These will be recorded locally using a digital scope. At the end of a plasma shot cycle, the data from the local digital scopes will be transferred to the QUEST data archival system.

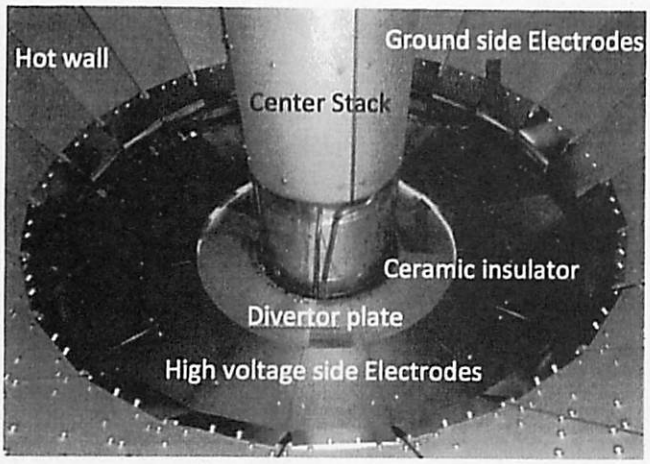

Figure 3: Photo of the top of the CHI electrodes. The CHI insulators are located between the divertor plates and the electrodes.

A detailed document summarizing the technical specifications of CHI capacitor bank, the snubber, the gas injection system, the capacitor bank and gas injection systems control logic is now in the final stages of completion. The experimental testing and operations of CHI on QUEST will take place in two parts.

PART A: The first part will commission the entire system. First, the gas injection system will be tested and calibrated. Then, we will apply 2-3 kV to the current feed rod, using a high voltage megger to verify the system voltage isolation capability. Such a test at the 1 kV level has already been conducted. This will be followed by operating the capacitor bank using the LabView based control software. During this dummy load test, the current feed rods will be shorted out.

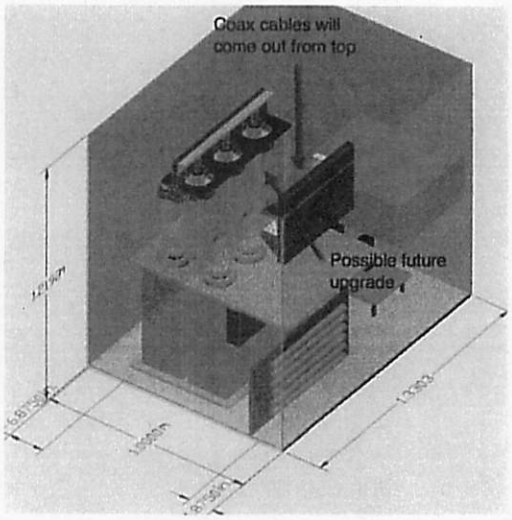

Figure 4: Conceptual view of the CHI capacitor bank. It will consist of two 10 mF, 2kV capacitor modules, each connected to a large ignitron. The two modules can be triggered at different times, to control the growth of the transient CHI discharge.

PART B: This will be a test of the capability of the system to correctly initiate a transient CHI discharge. The following steps are involved.

- Use a high value of the injector flux, so as to keep the CHI plasma near the injector.
- Inject gas from one valve and apply increasing amounts of voltage to test gas breakdown and plasma generation.
- Using a fast camera and other visible diagnostics we will verify that the discharge is occurring on top of the divertor plate, and in the correct location.
- If, necessary we will use ECH as a pre-ionization system.
- We will then reduce the injector flux, and grow the plasma into the vessel.
- This will be followed by establishing the correct coil currents needed in the other coils to provide equilibrium to the resulting transient CHI plasma.

国際化推進共同研究概要

No.7

タイトル：Thermal emission measurements with phased array technique

研究代表者：SHEVCHENKO, Vladimir

所内世話人： 出射 浩

来訪期間： 2015 年 2 月 24 日 ～ 2 月 27 日

概要：

QUEST では電子バーンシュタイン波輻射計測のために、９素子の導波管アンテナからなら位相配列アンテナが開発され、放射電界特性から良好な動作が確認されてい る。MAST でも同様なアンテナが用いられており、他の研究課題のワークショップに併せて研究打ち合わせを行った。電子バーンシュタイン波輻射は、電子バーンシュタイ ン波（静電波）と電子サイクロトロン波（電磁波）とのモード変換を経て観測されるため、輻射計測を用いて、加熱・電流駆動で必要となるモード変換過程を精 査することができる。MAST で観測されたモード変換窓の最新の解析結果等も議論された。

Thermal emission measurements with phased array technique

CCFE, Culham Science Centre, UK,Vladimir Shevchenko

Statement of goals and objectives:

The objective of this bidirectional research is aimed at developing a microwave imaging technique using remote sensing by an array of antennas to measure electron cyclotron/Bernstein emission (ECE/EBE) from high temperature plasma confined in toroidal geometry. In the QUEST project in Japan, such measurement is being developed using a phased waveguide antenna array and at the MAST project in the UK, special Vivaldi antennas are employed using a synthetic aperture imaging technique. The present collaboration is helpful in strengthening our understanding and sharing common problems and issues regarding such diagnostics.

Diagnostic objectives:

The mode converted Electron Bernstein Wave (EBW) heating and current drive is one of the most attractive possibility for steady state operation of spherical tokamaks. In QUEST, the O-X-B mode conversion scenario is employed, where efficient mode conversion is critically dependent on the optimal launch angle of the O-mode wave launched to its cut-off layer and the density gradient present there. The optimum injection angle of the heating wave can be determined by finding the viewing angle that maximizes the thermal emission intensity in the over dense plasma. This can be done through the radiometric measurements of this emission. The thermal emission measurement will be useful to study plasma turbulence and temperature fluctuations. Additionally, it can be envisaged for active interlock of high power auxiliary systems in future fusion reactors.

Diagnostic details:

A new 9 element [3x3] Phased Array Antenna (PAA) system has been developed for plasma diagnostics with reflectometry and EBW radiometry in QUEST [1, 2]. Figure 1 shows the field $E_x(x)$ and $E_y(x)$ intensity and phase profiles measured at the low power test facilities. The phase differences between 9 elements were adjusted to obtain an oblique viewing beam of 8 GHz for EBW radiometry at z = 0.2 m. The field intensity and phase profiles calculated using Kirchhoff integral code were also plotted. The measured fields in the oblique propagation were in good agreement with the calculated fields. Figure 2 shows contour plots of $E_x(x)$ and $E_y(x)$ intensity distributions. There were no serious side-lobes with more than -20 dB level. This 9 element PAA system has been used for reflectometry and EBW radiometry in QUEST. Since we had significant progresses on the antenna development, a meeting was arranged for discussion. This meeting was held within the framework of the RIAM workshop on " RF-only ST plasma confinement, sustainment, and interactions with wall materials" submitted by Prof. M. Peng. In addition to the EBW radiometry subject, some EBWH/CD effects in superposed 8.2 and 28 GHz injections on QUEST were discussed. The density was increased by spontaneous jumps up to the over dense state for the 8.2 GHz. The electron temperature was increased in the over dense

plasma. Plasma equilibrium with energetic electrons carrying the plasma current was discussed in association with EBW radiometry in over dense plasma.

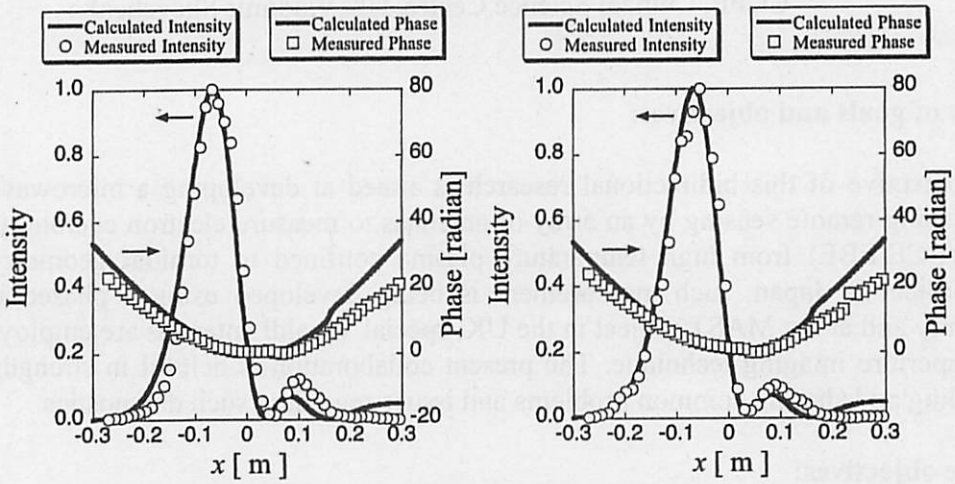

FIG1. : Field $E_x(x)$ and $E_y(x)$ intensity and phase profiles measured at the low power test facilities at propagating distance of z = 0.2 m. The beam was radiated from a new 9 element [3x3] Phased Array Antenna (PAA) system. The calculated field distributions were evaluated using Kirchhoff integral and also plotted.

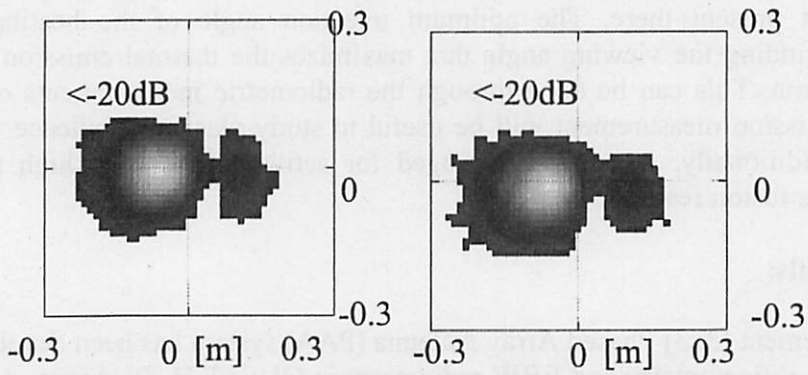

FIG2. : Contour plots of $E_x(x)$ and $E_y(x)$ intensity distributions for the profiles shown in FIG.1.

In the MAST tokamak synthetic aperture microwave imaging (SAMI) operates on the regular basis [3]. It delivers plasma images every shot at 16 different frequencies within the range from 10 to 34.5 GHz. Plasma is typically over dense ($\omega_{pe}>>\omega_{ce}$) in MAST so conventional EC emission is obscured by cut-offs while the mode converted EBW emission is clearly observed in majority of plasma shots. Figure 3 compares the 2D image of the EBW emission predicted by full wave modeling based on experimentally obtained plasma equilibrium and electron temperature profile and the image reconstructed from SAMI phased array measurements. Both images represent the plasma within the angular range visible from the low field side of the machine which is ±40° vertically and horizontally. Typically excellent agreement between modeling and experimental images is observed at relatively low densities. At high densities and during H-mode experimental images are often distorted by plasma flows.

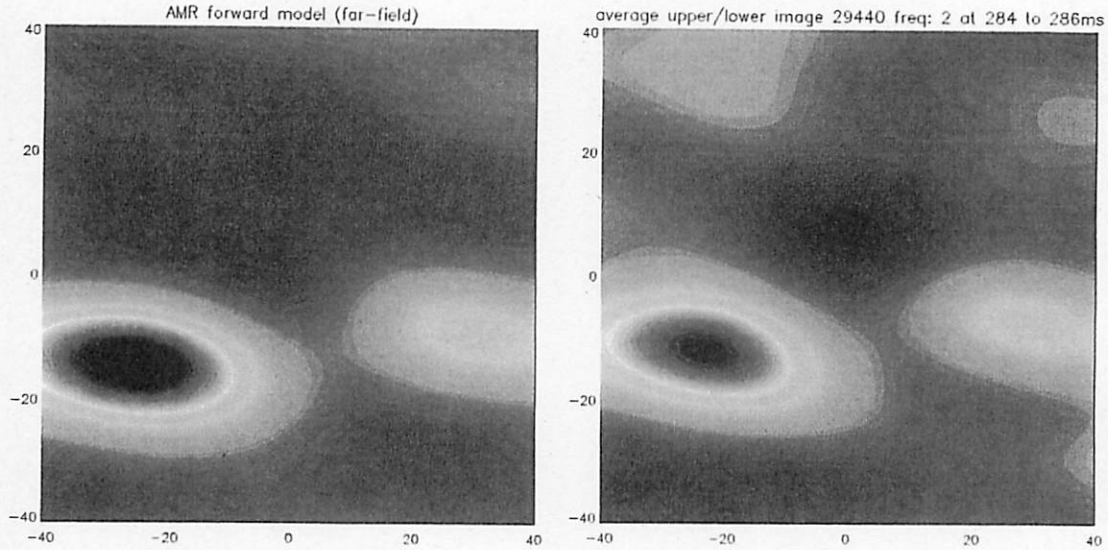

FIG. 3 Left: Contour map of B-X-O mode converted EBW thermal emission predicted by EBW ray-tracing and full wave coupling (AMR code) for the MAST shot #29440;
Right: Actual image of thermal plasma emission measured in the same shot by synthetic aperture microwave imaging (SAMI) at 11 GHz.

References:

1. H. Idei et al, Rev. Sci. Instrum. 85(11), 11D482 (2014)
2. K. Mishra et al, Rev. Sci. Instrum. 85(11), 11E808 (2014)
3. V. Shevchenko et al, Journal of Instrumentation, JINST 7, P10016 (2012)

国際化推進共同研究概要

No.8

タイトル：Numerical calculations for the PDP using PdCu membrane

研究代表者：SHARMA, SANJEEV, KUMAR

所内世話人： 図子 秀樹

来訪期間： 年 月 日 ～ 月 日

概要： S. K. Sharma 同氏とはメールを用いたデータ解析を行った。 というのも 研究所より長期の米国研究所（DIII）での中性粒子ビーム加熱に関するハードに関する出張が予定されており、米国側との実験等の予定打ち合わせが長引き、結局年度ぎりぎりまで半年以上の長期出張となった。このため九大への新たな出張が研究所から認められず、2015 年度早々に実施することにした。メールでの解析内容は こちらで取得したH透過束プローブデータの数値計算であり、同氏が九大時代に作成した計算コードでの解析である。今回の目的は拡散方程式を解くことにより 初期条件である入射束の時間発展と絶対値を決定する作業である。

1)トリチウム国際会議論文

Atomic Hydrogen Flux Measurement using Permeation Probes in Steady State QUEST Spherical Tokamak Plasma

A. Kuzmina,*, H. Zushia, I. Takagib, S. K. Sharmac, A. Rusinova, Y. Inoued, Y. Hirookae, H.Zhouf, M. Kobayashie, M. Sakamotog, K. Hanadaa, T. Onchia, N. Yoshidaa, K. Nakamuraa, A. Fujisawaa, K. Matsuokaa, H. Ideia, Y. Nagashimaa, M. Hasegawaa, S. Tashimad, S. Banerjeed, K. Mishrad

a)RIAM, Kyushu University, Kasuga, Fukuoka, 816-8580, Japan; * kuzmin@triam.kyushu-u.ac.jp

b)Kyoto University, c)Institute for Plasma Research, India, d)IGSES, Kyushu University, e)National Institute for Fusion Science, f)The graduate University for Advanced Studies g)Tsukuba University

2)Journal of Nuclear Materials 誌 online 掲載済み(2014)

Global gas balance and influence of atomic hydrogen irradiation

on the wall inventory in steady-state operation of QUEST tokamak

A. Kuzmin a,1,⇑, H. Zushi a, I. Takagi b, S.K. Sharma c, A. Rusinov a, Y. Inoue d, Y. Hirooka e, H. Zhou f,

M. Kobayashi e, M. Sakamoto g, K. Hanada a, N. Yoshida a, K. Nakamura a, A. Fujisawa a, K. Matsuoka a,

H. Idei a, Y. Nagashima a, M. Hasegawa a, T. Onchi a, S. Banerjee d, K. Mishra d

a RIAM, Kyushu University, 6-1 Kasugakoen, Kasuga, Fukuoka 816-8580, Japan

b Graduate School of Engineering, Kyoto University, Japan

c Institute for Plasma Research, Ahmadabad, Gujrat, India

3)FEC国際会議論文

Determination of the system function for the particle circulation process using perturbation technique in QUEST

H. Zushi, A. Kuzmin, I. Takagi[1)], S.K. Sharma[2)], M. Hasegawa, M. Kobayashi[3)], Y. Hirooka[3)], N. Yoshida, A. Rusinov[4)], A. Inoue[4)], H. Zhou[3)],A. Fujisawa, K. Hanada, H. Idei, K.

Nakamura, Y. Nagashima, K. Matsuoka[3], T. Onchi, S. Tashima[4], S. Banerjee[4], M. Sakaguchi[4], E. Kalinnikova[4], K. Mishra[4], X. Liu[4],S. Kubo[3], Y. Ueda[5], T. Fujita[6], S. Ide[7], N. Ohno[8], A. Hatayama[8], A. Ejiri[9], T. Yamaguchi[9],J. Hiratsuka[9], H. Togashi, [9]Y. Takase[9], A. Fukuyama[1], O. Mitarai[10]

Research Institute for Applied Mechanics, Kyushu University, Kasuga, 816-8580, Japan

[1] *Kyoto University,* [2] *IPR India,* [3]*National Institute for Fusion Science (NIFS), Gifu, Japan* [4] *IGSES, Kyushu University, Kasuga, 816-8580, Fukuoka, Japan,* [5] *Osaka University,* [6] *Nagoya University*[7] *Japan Atomic Energy Agency (JAEA), Ibaraki,* [8] *Keio University,* [9] *The University of Tokyo, Japan,* [10] *Tokai University,*

として公表された。

国際化推進共同研究概要

No.9

タイトル: Measurement of plasma flow and edge turbulence and their effect on plasma equilibrium in QUEST

研究代表者:BANERJEE, SANTANU

所内世話人: 図子 秀樹

来訪期間: 2014年6 月7 日 ～ 6 月 22 日

概要： 2014年6月に来日し、高速カメラを用いた揺らぎ計測に関する論文の打ち合わせを行った。refereeからのコメントに関する
議論を行い再投稿の結果以下のように受理掲載された。

Physics of Plasmas (1994-present) 21, 072311 (2014); doi: 10.1063/1.4890359
Role of stochasticity in turbulence and convective intermittent transport at the scrape
off layer of Ohmic plasma in QUEST
Santanu Banerjee, H. Zushi, N. Nishino, K. Hanada, M. Ishiguro, S. Tashima, H. Q. Liu, K. Mishra, K. Nakamura
, H. Idei, M. Hasegawa, A. Fujisawa, Y. Nagashima, and K. Matsuoka

compact toroid の入射に関して PIV 法の適用をカメラのイメージに対して行う実験を実施した。
実験データ取得後 年末に論文を投稿し、本年初めに受理された。

accepted for publication in Reviews of Instrument (2015)

Dynamical programming based turbulence velocimetry for fast visible imaging of tokamak plasma

Santanu Banerjee[1a)], H. Zushi[2], N. Nishino[3], K. Mishra[4], T. Onchi[2], A. Kuzmin[2], Y. Nagashima[2], K. Hanada[2], K. Nakamura[2], H. Idei[2], M. Hasegawa[2] and A. Fujisawa[2]

国際化推進共同研究概要

No.10

タイトル: Retrieval of microphysical and radiative parameters of cirrus clouds from combined data of radar and lidar sounding

研究代表者:BOROVOY, ANATOLY, GEORGIEVICH

所内世話人: 岡本 創

来訪期間: 2014 年 11 月 15 日 ～ 11 月 23 日

概要:
巻雲を構成する氷粒子の光散乱特性を計算する手法を開発し、
ライダ後方散乱特性について解析し、衛星搭載ライダデータと比較を行った。
衛星観測から得られている値は、従来から知られている解析手法では説明できず、開発した新たな手法によって説明可能である事が示された。

No. 10. Retrieval of microphysical and radiative parameters of cirrus clouds from combined data of radar and lidar soundings

Institute of Atmospheric Optics, Rus.Acad. Sci., Prof. A.G. Borovoy

Aim:

Aim of the project is to modify and check jointly the algorithms for retrieval of microphysical properties of cirrus clouds based on the synergy use of CPR, lidar ATLID, and multi-spectral radiometer of EarthCARE. These algorithms have been developed by the RIAM team (Okamoto et al., 2010, Sato and Okamoto 2011) where radar signals were calculated by the reliable numerical methods (DDA, FTDT). However, there were no reliable methods to calculate light backscatter by ice crystals of cirrus clouds. Last years the IAO team has just developed such a method called the physical-optics approximation. The numerical results obtained for the lidar ATLID should be included in the retrieval algorithms.

The heads of the teams Prof. H. Okamoto and Prof. A. Borovoi began their joint development of this scientific direction when Prof. A. Borovoi was a visiting researcher in RIAM for 3 months in 2011.

Method:

The problem of light scattering by such large particles as ice crystals of cirrus clouds is a vibrant problem of the atmospheric optics that is just under developing. Here the standard methods for solutions to the exact Maxwell equations like the T-matrix method (Mishchenko, 2000), the finite-difference time-domain method FDTD (Ping Yang, 2003), and the dipole discrete approximation DDA (Yurkin, 2006) prove to be computationally expensive for the ice crystals of cirrus clouds. Recently, these methods were modernized as the Pseudo-spectral time-domain method (PSTD) (Ping Yang at al., 2013) and the Invariant embedding T-matrix method (Bi et al., 2014) but these methods are capable to solve the problem for the ice crystal of sizes up to 20 micrometers for the visible yet.

However, there is a method that is practically independent of the ratio of (particle size/wavelength) called the size parameter. This is the physical-optics method. It was begun by Borovoi et al. in 2003 and then it has been improving for last years. In particular, in the recent paper A. Borovoi, A. Konoshonkin, N. Kustova "The physical-optics approximation and its application to light backscattering by hexagonal ice crystals." Journal of Quantitative Spectroscopy & RadiativeTransfer v.146, 181–189, 2014, the team of this Joint Research Project have clarified the applicability limitations for the physical-optics approximation. Also, the conditions for reduction of the geometric-optics solutions to the physical-optics ones and vice versa have been obtained and illustrated.

Simulations:

1. Randomly oriented crystals

Ice crystals of cirrus clouds are usually assumed to be randomly oriented. Therefore this case is of most importance for interpretation of lidar data where only backscattering is detected. However at present the theoretical data concerning backscattering by randomly oriented crystals were practically absent in the literature except of a few and scarcely reliable data published in the paper L. Bi, P. Yang, G.W. Kattawar, B.A. Baum, Y.X. Hu, D.M. Winker, R. S. Brock, J. Q. Lu "Simulation of the color ratio associated with the backscattering of radiation by ice particles at the wavelengths of 0.532 and 1.064 mm," J. Geoph. Res. v. 114, D00H08, doi:10.1029/2009JD011759, 2009 .

The team of this Joint Research Project recently managed for the first time to simulate this problem for the hexagonal ice columns and plates. Here the fine angular structure of all elements of the Mueller matrix in the vicinity of the exact backward direction is first calculated and discussed. In particular, an approximate equation for the differential scattering cross section

is obtained. Its simple spectral dependence is discussed. Also, a hollow of the linear depolarization ratio around the exact backward direction inherent to the long hexagonal columns is revealed.

2. Quasi-horizontally oriented hexagonal ice plates

Lidar sounding of cirrus clouds often detects the cases of quasi-horizontally oriented plate-like crystals where the depolarization is small and the backscattering coefficient is maximal. In these cases, the backscattering characteristics have a lot of peculiarities which can be effectively used for retrievals of the microphysical parameters of ice crystals. However, in the literature, the backscattering characteristics of the quasi-horizontally oriented crystals there were absent. The team of the Joint Research Project has successfully simulated this problem for the hexagonal ice plates. In the recent paper A. Borovoi, A. Konoshonkin, N. Kustova, "Backscatter ratios for arbitrary oriented hexagonal ice crystals of cirrus clouds," Opt. Lett. v. 39, No. 19, 5788-5791, 2014, three dimensionless ratios widely used for interpretation of lidar signals, i.e. the color ratio, lidar ratio and depolarization ratio, have been calculated for hexagonal ice crystals of cirrus clouds as functions of their spatial orientation. The physical-optics algorithm developed earlier by the authors is applied. It is shown that these ratios are minimal at the horizontal crystal orientation. Then these quantities increase with the effective tilt angle approaching the asymptotic values of the random particle orientation. The values obtained are consistent with available experimental data. Moreover, these theoretical data allowed the team members to propose and explore a new method for detecting these crystals as it is described in the recent paper A. Borovoi, Y. Balin, G. Kokhanenko, I. Penner, A. Konoshonkin, N. Kustova, "Layers of quasi-horizontally oriented ice crystals in cirrus clouds observed by a two-wavelength polarization lidar," Opt. Exp. v. 22, No. 20, 24566-24573, 2014. Layers of quasi-horizontally oriented ice crystals in cirrus clouds are observed by a two-wavelength polarization lidar. These layers of thickness of several hundred meters are identified by three attributes: the backscatter reveals a sharp ridge while the depolarization ratio and color ratio become deep minima. These attributes have been justified by theoretical calculations of these quantities within the framework of the physical-optics approximation.

Results:

During visit by Prof. A. Borovoi to RIAM in 2014, some new simulations of the backscattering characteristics for quasi-horizontally oriented hexagonal ice plates have been performed under the condition that the ice water content in cirrus clouds is given according to the data obtained from the space-borne radars. These data allowed the team headed by Prof. H. Okamoto to modify their algorithms for retrieving cirrus microphysics from the combined data of lidar and radar sounding from space. A comparison of the modified retrieval algorithms with experimental data proves their reliability and perspective.

During the visit, Prof. A. Borovoi delivered two lectures at the RIAM seminars: "The physical optics approach for scattering properties of non-spherical particles" and "The lidar scattering properties of ice crystal particles".

国際化推進共同研究概要

No.11

タイトル: Japan-Korea Oceanography Seminar on Regional Oceanography and Atmospheric Sciences

研究代表者: Shin, Hong-Ryeol

所内世話人: 広瀬 直毅

来訪期間: 2014 年 5 月 15～16 日

概要: 〝Japan-Korea Oceanography Seminar on Regional Oceanography and Atmospheric Sciences〟を開催した。九州・山口地域の関係者および韓国の海洋系教員・学生など多数が参加し、小規模な乱流過程から大規模な気候変動まで多岐に渡る研究内容について活発に議論した。

Report of the International Joint Research Program in RIAM

Japan-Korea Oceanography Seminar on Regional Oceanography and Atmospheric Sciences

平成 26 年 5 月 15 日（木）－16 日（金）

九州大学応用力学研究所

Report of the Japan-Korea Oceanography Seminar on Regional Oceanography and Atmospheric Sciences

Shin, Hong-Ryeol (Kongju National University, Korea)
Takikawa, Tetsutaro (National Fisheries University)
Hirose, Naoki (RIAM, Kyushu University)

Aim of research

CREAMS プロジェクトに代表されるように、応用力学研究所は長年、東アジア縁辺海の海洋研究をリードしている。しかし近年、日本海（韓国名：東海）の呼称問題等の政治的影響からか、日韓の共同研究が縮小傾向にあり、特に若手の miscommunication が懸念される。 日韓それぞれの海洋学会間においても、呼称問題が足枷となり、協力関係を構築するのが困難な状況である。

そこで東アジア海洋の研究を活発に行っており、地理的にも日韓の接点となる九州大学応用力学研究所が、「日韓海洋学会」の 中核を担うことが期待される。特に対馬海峡の観測データや東アジア縁辺海データ同化モデルの解析値を活用することによって、日韓の領域的な海洋学の発展が望まれ、さらには環境問題や大気海洋相互作用まで波及効果が期待される。

九州大学付近で日本と韓国の海洋学者と若い学生が集まって、東アジア縁辺海の研究成果をワークショップで発表することで研究内容の意見交換及び国際交流を増進させることが出来るだろう。特に若い大学院生を育てる良い機会で、大学院の学生が英語で発表及び質疑応答をすることで国際的な感覚を身に付けることも出来る。

Abstract of your research project

応用力学研究所がリードしている日本海・東シナ海の海洋研究を中心的テーマとする。両海に代表される東アジア縁辺海の海水特性、海流構造とそれらの長期・短期的変動、気象との関連性に対して、観測と数値モデルの研究を推進する。さらに、北太平洋や河川水の影響、低次生態系の変化なども議論する。日韓フェリーに搭載した超音波 流速計(ADCP)データや水温・塩分・蛍光光度観測データを活用する。

Results

2014 年 5 月 15 日から 16 日にかけて、下関市海峡メッセ会議室において、"Japan-Korea Oceanography Seminar on Regional Oceanography and Atmospheric Sciences"を開催し

た。九州・山口地域の関係者および韓国の海洋系教員・学生など多数が参加し、初日に合計 13 件の講演があった（講演内容はプログラム参照）。その内容は、小規模な乱流過程から大規模な気候変動まで内容は多岐に渡る。一題あたり、質疑応答含む 25 分という十分な時間を割き、活発な議論が促進され、時には講演時間を超過することもあった。２日目は個別に共同研究の打ち合わせが行われた。日本（韓国）の教員が韓国（日本）の大学院生にアドバイスする貴重な機会となった。

セミナーの実施体制としては、韓国側は代表者(Prof. Shin, H.-R.)が、日本側は世話人（広瀬教授）が参加者を募り、水産大学校の滝川准教授が現地対応に当たり、この３名でプログラムを作成した。

日本海（東海）と東シナ海の海洋物理学を中心として、その環境問題や大気海洋相互作用などの周辺問題まで含めた課題について、各自が研究成果を発表し、さらなる問題点や今後の課題を掘り下げた。関釜フェリーの発着する下関市内にて研究集会を開催したため、交通費や宿泊費を節約でき、多数の若手（学生や PD）が参集した。実際に講演 13 件のうち 9 件は大学院生あるいは最近学位を取得したばかりの PD による話題提供であった。２日目は若手同士の意見交換が活発に行われ、日韓の若手研究者の交流促進に貢献できたといえるだろう。

Program

Thursday, May 15, 2014

09:30-09:40 Opening Address

09:40-10:05 Young Ho Seung (Inha University)
Why is the deep current asymmetric in the Ulleung Inter-plain Gap, East/Japan Sea?
10:05-10:30 Kenki Kasamo, Atsuhiko Isobe (RIAM, Kyushu University)
A climate teleconnection between JES and East China Sea mediated by the Kuroshio in winter
10:30-10:55 Hyejin Ok, Yign Noh, Eunjeong Lee (Yonsei University), Naoki Hirose (Kyushu University), Takahiro Toyoda (Meteorological Research Institute)
Effect of the Parameterization of Langmuir Circulation in the OGCM

11:10-11:35 Jae Ho Lee and Hong-Ryeol Shin (Kongju National University)
Comparison of geostrophic currents by using satellite-altimeter data and hydrographic data

11:35-12:00 Masashi Ito, Akihiko Morimoto (HyARC, Nagoya University), Yutaka Isoda (Hokkaido University), Tetsutaro Takikawa (National Fisheries University), Hiroyuki Tomita (Nagoya University)

Interannual variation in the third branch of the Tsushima Warm Current path controlled by winter surface cooling in the Japan Sea

12:00-12:25 Katsumi Takayama, Naoki Hirose (RIAM, Kyushu University), Tatsuro Watanabe, Haruya Yamada (Fisheries Research Agency)

Seasonal patterns of ocean current in the west of Kyushu analyzed by the JADE2 model results

14:30-14:55 Yasuyuki Miyao (ESST, Kyushu University), Atsuhiko Isobe (RIAM, Kyushu Univ.)

An application of low-altitude remote sensing using a vessel-towed balloon for monitoring fine structure around coastal fronts

14:55-15:20 Yuichi Iwanaka (ESST, Kyushu University), Atsuhiko Isobe (RIAM, Kyushu University), Shin'ichiro Kako (Kagoshima University)

Balloon-based remote sensing and non-hydrostatic modeling of frontal waves around an estuarine front

15:20-15:45 Dae Hyuk Kim and Hong-Ryeol Shin (Kongju National University)

Long-term variation of dissolved oxygen along 137 E line in the western north Pacific

15:45-16:10 Eunjeong Lee, Yign Noh (Yonsei University), Bo Qiu (University of Hawaii)

Seasonal Variation of the Upper Ocean Responding to Surface Heating in the North Pacific

16:20-16:45 Bin Wang, Naoki Hirose, Boonsoon Kang and Katsumi Takayama (RIAM, Kyushu University)

Seasonal migration of the Yellow Sea bottom cold water (YSBCW)

16:45-17:10 Boonsoon Kang and Naoki Hirose (RIAM, Kyushu University)

A non-isostatic response of sea level to synoptic pressure forcing in the Yellow Sea

17:10-17:35 Naoki Hirose (RIAM, Kyushu University), Atsushi Kaneda, Noriyuki Okei, Yutaka Kumaki, Kei-ichi Yamazaki, Tatsuro Watanabe

Prediction of rapid coastal current in the southern Japan/East Sea

Friday, May 16, 2014

Group disscussions on Japan-Korea cooperative research

国際化推進共同研究概要

No.12

タイトル: Generation and Propagation Dynamics of Nonlinear Internal Solitary Waves

研究代表者: LAMB, KEVIN, GRAHAM

所内世話人: 辻　英一

来訪期間: 2015 年 1 月 31 日 ～ 2 月 8 日

概要：　孤立波の大振幅二次元相互作用や海洋での不安定や混合の解明を目指した数値シミュレーションの結果と考察などについて情報交換や議論を行った。その結果、共同研究者らのこれまでの知見を活かし、連続成層モデルの方程式の解として報告されている breather と呼ばれる波動解に関連して、breather 同士の二次元相互作用について理論的・数値的に調べる共同研究を行うとの方向で一致した。

Generation and Propagation Dynamics of Nonlinear Internal Solitary Waves

Kevin Lamb and Hidekazu Tsuji

Internal wave in the ocean is a fundamental phenomenon for mixing and transport process. Observations reveal that the waves sometimes have very large amplitude (a few tens meter) and steadily propagate for a long time and distance.

Dr. Tsuji has been interested in nonlinear wave (especially solitary wave) and investigated horizontally two-dimensional interaction of the nonlinear waves. It is found that the interaction can produce very large amplitude wave. Prof. Lamb has studied the stability and mixing in the ocean and clarifies the various phenomena using model equations and global circulation model.

During the staying of Prof. Lamb in the institute, we have discussed our past and ongoing works in detail. By the discussion we both have much interest about the Gardner equation and one of its solutions: "breather".

The Gardner equation is a nonlinear model equation in certain kind of continuously stratified fluid. In the fluid with normal stratification, Korteweg-de Vries (KdV) equation is derived as a governing equation with the assumption of weak nonlinearity. The KdV equation has the second-order nonlinearity term and dispersive term. The coefficients of these terms are described by the structure of stratification. In some cases that the coefficient of the nonlinear term is very small the third-order nonlinearity must be taken to account. So the KdV equation is extended to the Gardner equation which has both the second and third order nonlinear term. Unlike KdV equation, Gardner equation has not only the soliton solution but also the "breather" solution which propagates with pulsating. Although there has been many researches about the breather solution, its behavior in horizontally two-dimension propagation is not yet studied.

At present we have the plan to investigate the two-dimensional interaction of the two breathers which propagate in the different directions. Especially it is interesting whether the remarkable amplification which is often observed in the interaction of two solitons can be found or not. The different type of the interaction, namely the interaction of a soliton and a breather can be also considered.

The result should be compared to the corresponding investigation of the fully nonlinear numerical calculation. It is noted that this comparison might be possible in the ongoing joint study supported in the institute (Prof. Kakinuma, Prof. Nakayama and Dr. Tsuji).

国際化推進共同研究概要

No.13

タイトル: International research collaboration on next generation thermo-electric and high frequency power devices developments.

研究代表者: REYNOLDS JR, William, Thomas

所内世話人: 寒川 義裕

来訪期間: 2015年 1月5日 ～ 1月12日

概要:

熱電変換・パワーデバイス開発に向けたRIAM国際研究集会

本研究集会ではバージニア工科大学(VT)材料工学科と九州大学
応用力学研究所・エネルギー基盤技術国際教育研究センター・
総合理工学府との表記課題に関する共同研究シーズの発掘を
行うことを目的として開催された。第1回目の今回は
VTからW. T. Reynolds Jr. 教授、G-Q. Lu教授を向かえ
固有量子熱力学と電子デバイスのパッケージングに関する
研究紹介を得た。また、応用力学研究所からH. Valecia学術研究員が
超高効率太陽電池の開発に関する研究紹介を行った。
関係機関における研究活動の相互理解が得られ共同研究の
開始に向けた礎を築くことができた。

RIAM International Workshop on Development of Thermoelectric and Power Devices

15:00-16:35, 8th January, 2015

Room W601, RIAM, Kyushu University

15:00-15:05

Opening address

Yoshihiro Kangawa (RIAM, Kyushu University)

15:05-15:35

Materials Science & Engineering at Virginia Tech and Synergistic Collaborations

William T. Reynolds Jr. (Department of Materials Science and Engineering, Virginia Tech)

15:35-16:05

Electronic Packaging Research for Power Electronics Integration

G-Q. Lu (Department of Materials Science and Engineering and The Bradley Department of Electrical and Computer Engineering, Virginia Tech)

16:05-16:35

III-V-N material design for high efficiency multi-junction solar cells: a theoretical model for the Vapor-Phase Epitaxy of $GaAs_{1-x}N_x$.

Hubert Valencia, Yoshihiro Kangawa, Koichi Kakimoto (RIAM, Kyushu University)

Materials Science & Engineering at Virginia Tech and Synergistic Collaborations

William T. Reynolds Jr.
Department of Materials Science and Engineering
Virginia Tech

This talk will provide an introduction to Virginia Tech and the University's Materials Science and Engineering Department. After describing how the faculty are organized, the focus of several research groups will be presented with the goal of highlighting areas of potential collaboration between Virginia Tech and Kyushu University. Among the research interests common to the two universities, materials behavior far from equilibrium is a possible unifying theme. At the atomistic level, classical and quantum mechanics are powerful tools for investigating the ground state energy of a system, but these tools provide no information about the non-equilibrium states that give rise to many useful properties. Intrinsic Quantum Thermodynamics is a relatively new field that shows promise for unifying atomistic behavior and classical thermodynamics without introducing the inconsistencies associated with statistical thermodynamics. A short introduction to the concepts underlying Intrinsic Quantum Thermodynamics will be presented along with some of its key advantages. In particular, incorporating entropy in the quantum framework makes it feasible to uniquely identify the path a system follows to reach equilibrium. Consequently, the approach has the capacity to provide predictive insights in systems far from equilibrium and in which quantum effects are important.

Electronic Packaging Research for Power Electronics Integration

G-Q. Lu, Professor
Department of Materials Science and Engineering and
The Bradley Department of Electrical and Computer Engineering
Virginia Tech
213 Holden Hall, Dept. of MSE, Virginia Tech
Blacksburg, VA 24061-0237
Tel: (540) 231-8686; E-mail: gqlu@vt.edu

Researchers in the field of power electronics continuously strive to improve efficiency and power density of switch-mode converters through circuit design and functional integration. Electronic packaging of power converters is critical for sustaining the technology trend of the field. Recent advances in wide bandgap semiconductor devices offer new challenges and opportunities for power electronic packaging. Innovative packaging technologies are needed to enable high switching frequency and reliable operation at high temperatures. A low-temperature silver sintering technology is emerging as a lead-free chip-bonding solution for high-reliability, high-temperature packaging of power electronics. However, one concerning issue with many of the silver

sintering die-attach processes is the requirement of large uniaxial stress, ranging from 10 MPa to 40 MPa, to reduce the sintering temperature below 250°C. In this presentation, I report our findings in the evaluation of a nanosilver paste technology developed to eliminate pressure needed for the silver-sintering process. The nanosilver paste can be readily stencilprinted or dispensed for chip interconnection at temperature below 250°C in air or controlled atmosphere under zero mechanical force. Findings on the sintering behavior of the nanosilver paste and properties of the sintered joints will be presented. As a specific application example, the nanosilver-enabled die-attach process was used to make planar power modules in which both sides of the IGBT chips were bonded by the sintered nanosilver joint.

III-V-N material design for high efficiency multi-junction solar cells: a theoretical model for the Vapor-Phase Epitaxy of GaAs1-xNx.

Hubert Valencia, Yoshihiro Kangawa, Koichi Kakimoto

III-V-N alloys, such as (In)GaAsN, present unique physical properties that make them the focus of a growing interest for optoelectronic devices and multi-junction solar cells. Especially for the latter, the incorporation of small amounts of N on GaAsN material significantly lower its band gap, making it a candidate of choice for multi-junction solar cells with very high efficiency. However, a high quality growth of (In)$GaAs_{1-x}N_x$ remains challenging due to the low miscibility of N in III-V alloys. Moreover, while many experimental analysis exists, little is known about the fundamental characteristics and reactions of this crystal growth process.

In this study, we examined GaAs(100) c4x4 surfaces using *ab initio* calculation under As_2, H_2 and N_2 gas mixed conditions as a model for GaAs(100) surface vapor-phase epitaxy of $GaAs_{1-x}N_x$. By performing As_2 and H_2 adsorptions and As/N substitutions on GaAs(100) c4x4 surface it was possible to obtain the relative stability diagram of resulting surfaces against chemical potential of As_2, H_2, and N_2 gas. Using this diagram with a simple model for decomposition of experimental precursors into our simple diatomic gases, we obtain a picture of the crystal growth behavior for several experiments, including metal-organic chemical vapor deposition (MOCVD) and chemical beam epitaxy (CBE). We found that several N-incorporation regimes were possible, depending on the nature of the experiment and its conditions, as observed experimentally. It was possible to reproduce with a good accuracy the conditions for the transition between these regimes and a rational explanation can be given regarding the efficiency of N-incorporation during each regime. Our model should then leads to a better comprehension of vapor-phase epitaxy of $GaAs_{1-x}N_x$, as well as a possible insight for the enhancement of high quality growth conditions.

国際化推進共同研究概要

No.14

タイトル: International research collaboration on theoretical and experimental methods for marine renewable energy development

研究代表者: ZHANG, Liang

所内世話人: 胡 長洪

来訪期間: 2015 年 1 月 30 日 ～ 2 月 1 日

概要： 今年度の国際化推進共同研究「International research collaboration on theoretical and experimental methods for marine renewable energy development」に関して，共同研究・研究集会とも予定通り実施しました。共同研究成果について，論文投稿を準備中である。研究集会について，世 話人が担当した特定研究の研究集会と共同開催で，外国から 26 名，日本から約 40 名の参加者があり，海洋エネルギー開発を行う研究者にとって有意義な国際 研究集会となった。

Report for 2014 RIAM International Joint Research Project

International research collaboration on theoretical and experimental methods for marine renewable energy development

Purpose

A new floating marine renewable energy system in which multiple wind turbines as well as solar panels, wave energy or ocean current energy converters are installed together on one floating body, has been proposed by the research group of RIAM and is receiving considerable attention in the world. Related researches have been carried out for several years. HEU is the pioneer university on marine renewable R&D in China. In recent years HEU is well known in the world by their tidal current converter's on-sea experiment. The purpose of this joint research is to provide a chance to discuss in detail and exchange know-how between the two research groups on marine renewable energy researches, especially on advanced theoretical and experimental methods in this research field.

Research Plan

Marine renewable energy devices are usually installed in a sea area where severe environmental conditions have to be considered. On the other hand, cost control is strictly required for those devices in order to pass economic evaluations. Therefore for design of the devices, high-performance numerical methods are required to predict the hydro- and aerodynamic loads on the devices. Therefore in this year, a collaborative research on validation of practical numerical methods for prediction of floating wind turbines is planned. Further, in the end of 2014, a research workshop will be held in RIAM related to this joint research project, in which the collaboration research results will be presented and extensive discussion with other researchers will be made.

Member

Researcher's Name	Name of University or Institute	Present Status or Grade (graduate students)	Researcher role
Liang Zhang	HEU, China	Professor	Representative person (tidal energy)
Qihu Sheng	HEU, China	Associate professor	Co-PI (offshore wind)
Xuewei Zhang	HEU, China	Lecturer	Co-PI (blade mechanics)
Yong Ma	HEU, China	Lecturer	Co-PI (mooring system)
Yusaku Kyozuka	Kyushu Univ.	professor	Co-PI (tidal energy)
Makoto Sueyoshi	RIAM, Kyushu Univ.	assistant professor	Co-PI (experiment)
Kangping Liao	RIAM, Kyushu Univ.	Posdoc	Co-PI (wave energy)
Changhong Hu	RIAM, Kyushu Univ.	Professor	RIAM Attendant

Summary of Collaboration Research

A collaboration research on coupled methods for spar-type offshore floating wind turbine system has been carried out in 2014. In this study, the non-linear time-domain coupled kinetic equations of the floating turbine system is established. The effect of steady wind and regular wave on the performance of a spar-type

offshore floating wind turbine is investigated and the overall motion response under random wave condition is also analyzed. Numerical simulation results demonstrate that constant wind affects the average and peak-to-peak values of surge, pitch, heave, sway and roll at the rated wind speed, and regular wave has marginal effects on the average values of surge, pitch, heave, sway and roll but enlarges their peak-to-peak values. Under the condition of random wind and waves, the system's surge motion is dominant in low frequency; on the other hand, the system's heave motion is significant for both low frequency and high frequency. Low frequency pitch motion is more obvious at the rated wind speed while high frequency pitch motion is more obvious at higher wind speed. The results of this study provide useful information for design of a spar-type offshore floating wind turbine system.

Summary of Research Workshop

In 2014 a designated joint research program of RIAM was launched with the subject "R&D on Multipurpose Floating Structure for Marine Renewable Energy", in which a workshop on "Development of Floating Marine Renewable Energy Systems" is included. The objective of this workshop is to provide a forum for relevant researchers to present new results and exchange ideas on ocean renewable energy technologies. The workshop proposed in this international joint research project workshop is held jointly with above mentioned designated joint research workshop.

The research budget provided for this international joint research has been used to support travel expenses of the following 4 scholars to the workshop.

1. Liang Zhang, Professor of Harbin Engineering University, China
2. Decheng Wan, Professor of Shanghai Jiao Tong University, China
3. Xuewei Zhang, Lecturer of Harbin Engineering University, China
4. Yong Ma, Lecturer of Harbin Engineering University, China

On the workshop, these invited scholars have presented their recent researches on ocean renewable energy development, and have discussed with participates from Japan and other countries. The program of the workshop is as follows.

Date: December 19-20, 2014
Place: W601, RIAM, Kyushu University

TIME TABLE

19 December (Friday)

13:00 - 13:10	Opening Address Yuji Ohya (Director, RIAM, Kyushu University, Japan)
13:10 - 14:00	*Keynote Invited Lecture* Numerical and experimental strategies for tidal turbine farms design Pierre Ferrant (Director, LHEEA Lab, Ecole Centrale de Nantes, France)
14:00 - 14:50	*Keynote Invited Lecture* Offshore Wind Energy in the US and the Development of new IEC Design Standards for Offshore Wind Turbines James Manwell (Director, Wind Energy Center, University of Massachusetts, USA)

14:50 - 15:00	Coffee break
15:00 - 15:30	Downwind Rotor Technologies for Offshore Wind Turbines Shigeo Yoshida (Kyushu University, Japan)
15:30 - 16:00	Numerical Simulations of Offshore Wind Turbine Wake Flows and its Supported Floating Platform Flows Decheng Wan (Shanghai Jiao Tong University, China)
16:00 - 16:30	A Preliminary Design and Performance Estimation of an Ocean Current Turbine Kohei Tokunaga, Hidetsugu Iwashita (Hiroshima University, Japan)
16:30 - 17:00	CFD Simulation of a Horizontal Axis Tidal Turbine based on OpenFOAM Cheng Liu, Changhong Hu (Kyushu University, Japan)
17:00 - 17:30	Development of accurate and practical unstructured-grid model for interfacial multi-phase fluid dynamics Feng Xiao, Bin Xie (Tokyo Institute of Technology, Japan)

20 December (Saturday)

9:00 - 9:30	Numerical and experimental study of the aero/hydrodynamics of FOWT in HEU Liang Zhang (Harbin Engineering University, China)
9:30 - 10:00	Prescreening of environmental conditions for dynamic analysis of floating structures Dong-Hyun Lim, Taeyoung Kim, Yonghwan Kim (SNU, Korea)
10:00 - 10:30	Precition of springing-induced tension on TLPs Taeyoung Kim, Yonghwan Kim (SNU, Korea)
10:30 - 11:00	Characteristics of Motions of a Floating Body for Offshore Wind Power Generation Kyohei Kajino, Hidetsugu Iwashita, Yasushi Higo (Hiroshima University, Japan)
11:00 - 11:30	Hydrodynamic prediction of FOWT with multiple wind-lens turbines Yingyi Liu, Changhong Hu (Kyushu University, Japan)
11:30 - 12:00	Conversion efficiency of Backward Bent Duct Buoy Yasutaka Imai (Saga University, Japan)
12:00 - 13:00	Lunch
13:00 - 13:30	Measurement of sloshing flows using Particle Image Velocimetry Jieung Kim, Sang-Yeob Kim, Yonghwan Kim (SNU, Korea)
13:30 - 14:00	Zero scattered-wave energy and wave pattern in cloaking phenomenon Takahito Iida, Mariko Miki, Masashi Kashiwagi (Osaka University, Japan)
14:00 - 14:30	Development of an ocean current turbine at OIST Katsutoshi Shirasawa, Tsumoru Shintaki (OIST, Japan) Kohei Tokunaga, Hidetsugu Iwashita (Hiroshima University, Japan)
14:30 - 15:00	Offshore wind farm experiment using Wind-lens turbines Tomo Nagai (Kyushu University, Japan)
15:00 - 15:30	Recent Progress of Tidal Current Power Projects in Japan Yusaku Kyozuka (Kyushu University, Japan)
15:30 - 15:40	Closing Remarks Hidetsugu Iwashita (Hiroshima University, Japan)

国際化推進共同研究概要

No.15

タイトル：Effects of compaction on interlaminar fracture toughness of laminated CFRP composites fabricated by vacuum-assisted resin-transfer molding

研究代表者：CHOI, Nak-Sam

所内世話人： 新川 和夫

来訪期間： 2015年2月1日 ～ 2月4日

概要：
真空樹脂含浸（VARTM）法を応用し、炭素繊維強化複合材料（CFRP）を作製した。CFRP板より、三点曲げ試験片、またテフロンフィルムを層間に挿入することにより、初期き裂を導入した試験片を作製した。得られたCFRPの層間破壊挙動をアコーステックエミッション（AE）法を用いて計測し、積層形態や枚数依存性などを明らかにした。

Springer

KSME

Journal of Mechanical Science and Technology 29 (1) (2015) 17~21
www.springerlink.com/content/1738-494x
DOI 10.1007/s12206-014-1203-2

AE analysis of delamination crack propagation in carbon fiber-reinforced polymer materials †

Sang-Jae Yoon[1], Dingding Chen[2], Seung-Wook Han[3], Nak-Sam Choi[4] and Kazuo Arakawa[1,*]

[1]*Research Institute for Applied Mechanics, Kyushu University, Kasuga-koen 6-1, kasuga, Fukuoka, 816-8580, Japan*
[2]*College of Basic Education for Commanding Officers, National University of Defense Technology, 410073 Changsha, China*
[3]*Department of Mechanical Engineering, Graduate School, Hanyang University, Seongdong, Seoul, 133-791, Korea*
[4]*Department of Mechanical Engineering, Hanyang University, Sangrok, Ansan, 426-791, Korea*

(Manuscript Received April 1, 2014; Revised May 23, 2014; Accepted June 2, 2014)

Abstract

Delamination fracture behavior was investigated using acoustic emission (AE) analysis on carbon fiber-reinforced polymer (CFRP) samples manufactured using vacuum-assisted resin transfer molding (VARTM). CFRP plate was fabricated using unidirectional carbon fiber fabric with a lay-up of six plies $[+30/-30]_6$, and a Teflon film was inserted as a starter crack. Test pieces were sectioned from the inlet and vent of the mold, and packed between two rectangular epoxy plates to load using a universal testing machine. The AE signals were monitored during tensile loading using two sensors. The average tensile load of the inlet specimens was slightly larger than that of the vent specimens; however, the data exhibited significant scattering due to non-uniform resin distribution, and there was no statistically significant different between the strength of the samples sectioned from the inlet or outlet of the mold. Each of the specimens exhibited similar AE characteristics, regardless of whether they were from the inlet or vent of the mold. Four kinds of damage mechanism were observed: micro-cracking, fiber–resin matrix debonding, fiber pull-out, and fiber failure; and three stages of the crack propagation process were identified.

Keywords: Acoustic emission (AE) analysis; CFRP composite; Damage mechanism; VARTM process

1. Introduction

Laminated composite materials have been applied in a variety of structural engineering fields, including aerospace, wind power plants, and the automotive industry. Conventional composite parts are typically manufactured using an autoclave method with unidirectional pre-preg composite fibers; however, autoclaves incur substantial installation costs and it is difficult to fabricate composite parts with complex shapes. Vacuum-assisted resin transfer molding (VARTM) is a composite fabrication process in which a thermoset resin is injected into a mold through inlet ports, and the core materials contained in the mold are saturated with the resin. This process can save both cost and processing for curing compared with the autoclave method because high pressures and temperatures are not required, and complex parts can be fabricated to reduce the number of parts required [1]. For these reasons, VARTM has become an increasingly popular method to fabricate carbon fiber-reinforced polymer (CFRP) parts.

The Research Institute for Applied Mechanics of Kyushu University in Japan has developed a new wind-lens turbine to generate high output power using a diffuser [2]. The research group plans to increase the size of the wind-lens turbine to a 5-MW class. The parts required for this are very large, and the wind turbine is composed of many curved components. The VARTM process is a promising method to fabricate these parts.

The VARTM process has three basic steps: fiber impregnation, consolidation (i.e., the application of pressure), and curing [3]. In this process, the contact quality of all layers is influenced by several factors, including the mold temperature, fiber orientation, resin viscosity, and pressure in the mold [4-8]. However, significant defects may occur depending on the local pressure gradient and permeability of the fabrics in the mold [9]. Moreover, incomplete filling of the resin may degrade the mechanical properties of the product due to the creation of voids and other non-uniformities in the resin distribution. Therefore, it is important to determine the optimal resin flow and to control the resin flow, as well as to investigate the causes of defects.

Various studies have reported optimal VARTM process conditions. Johnson [9, 10] applied an induction heating

*Corresponding author. Tel.: +81 92 583 7761, Fax.: +81 92 583 3947
E-mail address: k.arakaw@riam.kyushu-u.ac.jp
† This paper was presented at the FEOFS 2013, Jeju, Korea, June 9-13, 2013.
Recommended by Guest Editor Jung-Il Song

Table 1. Maximum load prior to failure for each specimen.

Specimen type	No.	Maximum force (N)	Specimen type	No.	Maximum force (N)
Inlet	1	216	Vent	1	222
	2	192		2	199
	3	207		3	213
	4	239		4	209
	5	210		5	187
	Average	212.8		Average	206

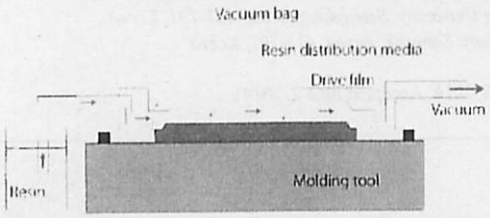

Fig. 1. Schematic diagram showing the VARTM process.

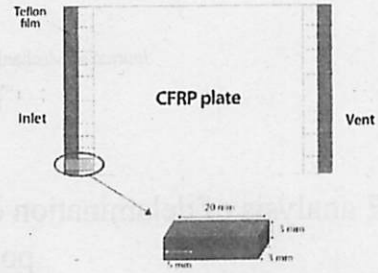

Fig. 2. Illustration showing where the specimens were sectioned from the CFRP plate.

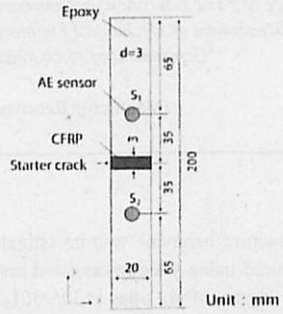

Fig. 3. Experimental tensile testing and AE monitoring procedures.

method to reduce the viscosity of the resin, thereby counteracting the effects of localized regions of low permeability, and simulated active flow control during the mold filling stage. Bender [11] reported an automatic pressure control and flow rate feedback method employing computer control between the inlet and vent parts. Correia [12] described a simulation analysis for the flow, compaction, and permeability. Kuentzer [13] explored the resin bleeding and flow resistance of the void content within fiber tows experimentally and via numerical simulations. Lee [14] investigated the effects of the fiber direction on the resin flow direction. However, most of these studies focused on process control. The effects of non-uniformities on the mechanical properties of the VARTM-formed composite materials have not been investigated in detail.

Here, we describe the results of a study of the effects of non-uniformities on composite materials by forming CFRP plates using VARTM. Specimens for tensile testing were formed with a starter crack inserted in the CFRP plate, and sections were examined from the inlet and vent of the mold. Acoustic emission (AE) signals were monitored during the tensile fracture tests. The fracture surface was observed following the tests, and the AE characteristics were analyzed to investigate the fracture behavior of the specimens. Three stages of the fracture behavior were identified from the amplitudes and frequency spectra of the AE signals.

2. Experimental procedure

2.1 VARTM process

Laminated composite specimens with a single edge notch were fabricated using the VARTM process. Fig. 1 shows the transverse flow VARTM setup, which is commonly employed in the fabrication of very large parts [1]. Unidirectional carbon-fiber fabrics (SAERTEX) were laid up in a one-side mold with a sequence of $[+30/-30]_6$. Teflon film was inserted as a starter crack in two edges of the plate, as shown in Fig. 2. The fabrics were sealed in a vacuum bag, and then the resin (Nagase ChemetX) was impregnated into the fiber layers using the vacuum. The process was carried out at room temperature.

2.2 Tensile specimens

To fabricate the tensile test specimens, ten pieces were sectioned from the inlet and vent of the plate, as shown in Fig. 2. The pieces were packed between two rectangular epoxy plates to clamp the specimens to a universal tensile testing machine (Zwick 250, testXpert), as shown in Fig. 3.

3. Results and discussion

3.1 Tensile fracture test and AE analysis

Figs. 4(a) and (b) show typical tensile loads and amplitudes of the AE signal as functions of time for the specimens sectioned at the inlet and vent of the mold, respectively. The tensile loads are listed in Table 1. Although the average tensile load of the inlet (212.8 N) was slightly larger than that of the vent (206 N), the data exhibited significant scattering, and as such, there was no statistically significant difference between the tensile strength of the parts formed at the inlet and the vent. Johnson [8, 9] suggested that mold-filling during VARTM is a

Table 2. Amplitude and peak frequency of the AE signals during each stage.

Stage	Amplitude (mV)	First peak frequency (kHz)
I	5 - 50	130 - 170
II	10 - 40	150 - 250
III	500 - 10000	120 - 250

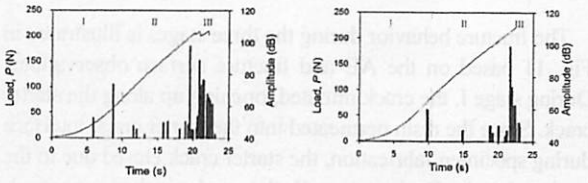

(a) (b)

Fig. 4. Load-displacement curves and the corresponding AE amplitudes as a function of time for specimens sectioned from (a) the inlet; (b) the vent regions of the mold.

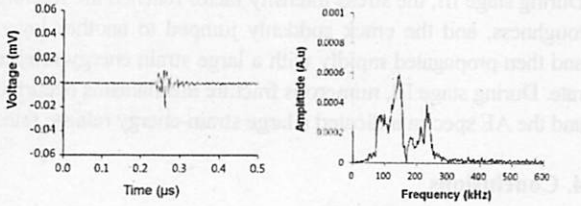

(a) (b)

Fig. 5. Burst-type AE signals during stage I of fracture: (a) waveform; (b) frequency spectrum.

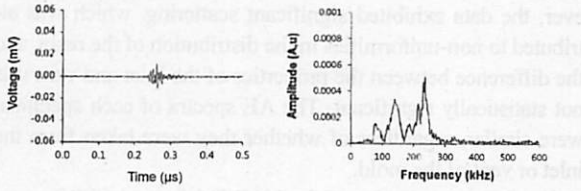

(a) (b)

Fig. 6. Burst-type AE signals during stage II of fracture: (a) waveform; (b) frequency spectrum.

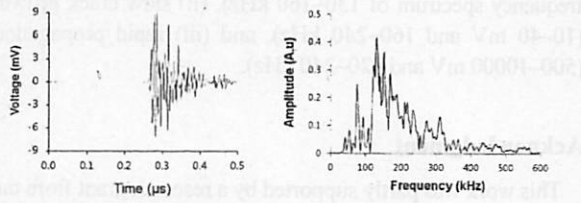

(a) (b)

Fig. 7. Burst-type AE signals (with a large amplitude) during stage III of fracture: (a) waveform; (b) frequency spectrum.

critical step in the process, and that defects often arise in regions of local low permeability, or in regions that are too far from the inlet or vent. The variation in the tensile strength may also be affected by non-uniformities of the fabrication process. The specimens exhibited similar AE characteristics, regardless of whether they were sectioned from the inlet or vent of the mold. Based on these data, we were able to identify three stages of the fracture behavior, which will be discussed in the following subsection.

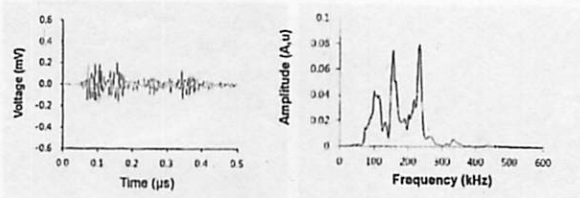

(a) (b)

Fig. 8. Continuous AE signals during stage III: (a) waveform; (b) frequency spectrum.

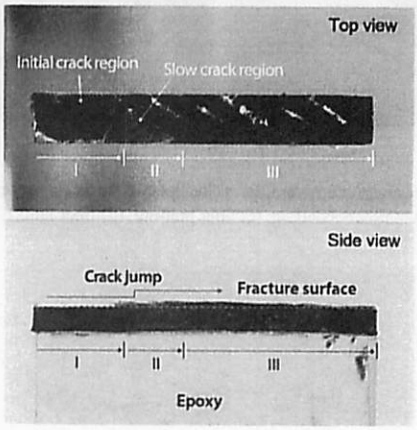

Fig. 9. Optical microscopy image of a fracture surface.

3.2 Fracture mechanism

The AE signals were analyzed in the time domain, as well as the frequency domain through the use of fast Fourier transforms (FFTs) of the time domain AE amplitudes. Figs. 5-8 show typical amplitude and frequency spectra of the AE signals during each stage of failure. Most of the AE signals exhibited a burst-type signal during fracture or crack growth, although continuous-type signals were observed during stage III (see Fig. 8). It should be noted that the crack propagation was significantly faster during stage III. Table 2 lists the distribution of the amplitudes and the frequency range of the lowest-frequency broad features in the AE signals. During stage I of failure, the samples exhibited low-amplitude AE signals, and most of the acoustic energy was at frequencies below 160 kHz. During stages II and III, the AE spectra exhibited wide bands at around 120–240 kHz.

Fig. 9 shows an optical microscopy image of a fracture surface. The three stages of crack propagation described above are marked on the fracture surface. During stage II, an area

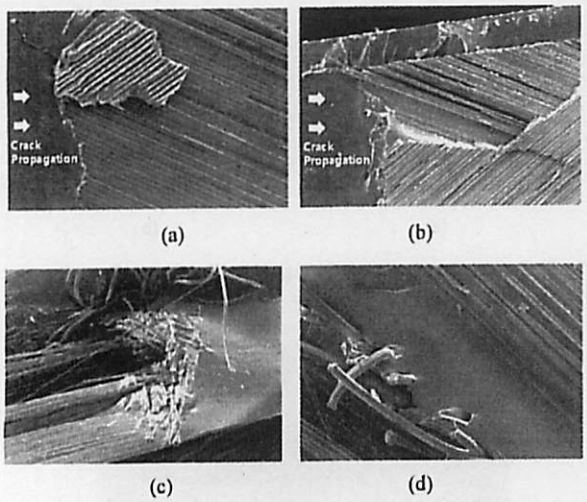

Fig. 10. SEM microscopy images of the fracture surfaces: (a) resin cracking; (b) fiber-matrix debonding; (c) fiber pull-out; (d) fiber failure.

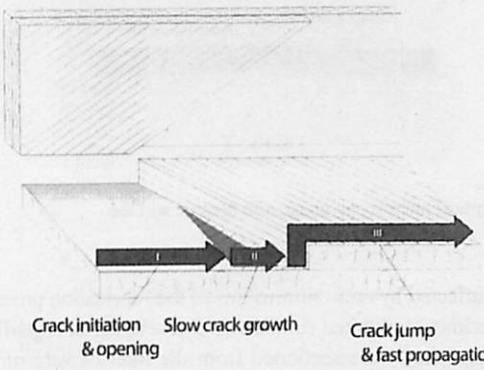

Fig. 11. Illustration of the fracture behavior in response to tensile loading.

corresponding to slow crack growth was observed. The fiber-bonded area was less than 80% delaminated opposite the fracture surface. This suggests that the matrix strength was stronger than the fiber-matrix strength, which corresponded to less than 80% of the bonded area.

At start of stage III, the crack propagation route changed to another layer. This stage was marked by a significant increase in the AE amplitudes (see Fig. 7). It follows that much energy was stored during the slow crack propagation of stage II, and that the crack suddenly jumped to the other layer, releasing a large amount of energy.

To further investigate the damage mechanism and to understand the relationship with the frequency spectra of the AE signals, scanning electron microscopy (SEM) images of the fracture surfaces were obtained. Fig. 10 shows four typical fracture phenomena at the fracture surface of the specimens, and Table 3 lists the phenomena that occurred during each stage. From a comparison with Table 2, the frequency band below 160 kHz appears to correspond to matrix-related fracture, and frequencies above 160 kHz correspond to fiber-related fracture.

Table 3. Observed damage mechanisms during each stage.

Stage	Phenomena
I	Resin cracking
II	Resin cracking, fiber-matrix debonding
III	Resin cracking, fiber-matrix debonding, fiber pull out, fiber failure

The fracture behavior during the three stages is illustrated in Fig. 11 based on the AE and fracture surface observations. During stage I, the crack initiated, opening up along the starter crack. Since the resin permeated into the starter crack interface during specimen fabrication, the starter crack closed due to the hardened resin. During stage II, the crack reached a poor adhesion area located at end of the starter crack. The crack propagated slowly until it reached fibers with at least ~80% of degree of adhesion. The crack propagation was temporarily restrained, and the strain energy accumulated at the crack tip. During stage III, the stress intensity factor reached the fracture toughness, and the crack suddenly jumped to another layer, and then propagated rapidly with a large strain energy release rate. During stage III, numerous fracture mechanisms occurred, and the AE spectra indicated a large strain-energy release rate.

4. Conclusions

Property non-uniformities of CRFP samples formed using VARTM were investigated using tensile testing and AE spectra. The tensile tests showed that average load of the inlet specimens was higher than that of the vent specimens; however, the data exhibited significant scattering, which was attributed to non-uniformities in the distribution of the resin, and the difference between the properties of the inlet and vent was not statistically significant. The AE spectra of each specimen were similar, regardless of whether they were taken from the inlet or vent of the mold.

The fracture behavior of the VARTM-formed CFRP material was investigated under tensile load. Failure could be classified into three stages: (i) crack initiation and opening along the starter crack (with an AE amplitude of 5-50 mV and a frequency spectrum of 130–160 kHz), (ii) slow crack growth (10–40 mV and 160–240 kHz), and (iii) rapid propagation (500–10000 mV and 120–240 kHz).

Acknowledgment

This work was partly supported by a research grant from the Japan Society for Promotion of Science (#26630496), and by the Collaborative Research Program of Research Institute for Applied Mechanics, Kyushu University.

References

[1] Y. Rachmadini, V. TAN and T. TAY, Enhancement of mechanical properties of composites through incorporation

of CNT in VARTM - A review, *J Reinf Plast Comp*, 29 (18) (2010) 2782-2807.

[2] Y. Ohya and T. Karasudani, A shrouded wind turbine generating high output power with wind-lens technology, *Energies*, 3 (4) (2010) 634-649.

[3] A. Miravete, *Processing and manufacturing composite design tutorial*, Aero/Astro Department, Stanford University (2007).

[4] J. L. Zhao, T. Fu, Y. Han and K. W. Xu, Reinforcing hydroxyapatite/thermosetting epoxy composite with 3-D carbon fiber fabric through RTM processing, *Mater Lett*, 58 (2004) 163-168.

[5] J. F. Timmerman, B. S. Hayes and J. C. Seferis, Nanoclay reinforcement effects on the cryogenic microcracking of carbon fiber/epoxy composites, *Compos Sci Technol*, 62 (2002) 1249-1258.

[6] J. Bozza, M. Erdal and S. Guceri, Resin transfer molding of continuous fiber-reinforced, particle-filled ceramic–ceramic composites: particle filtration, *In: Proceedings of the 28th international SAMPE technical conference* (1996).

[7] A. Haque, M. Shamsuzzoha, F. Hussain and D. Dean, S2-glass/epoxy polymer nanocomposites: manufacturing, structures, thermal and mechanical properties. *J. Mater. Sci. Lett.*, 20 (2003) 1439-1441.

[8] S. W. Han, N. S. Choi and M. S. Lee, Analysis of glass fabric impregnation using a resin drop method, *J. Mech. Sci. Technol.*, 26 (5) (2012) 1477-1482.

[9] R. Johnson and R. Pitchumani, Enhancement of flow in VARTM using localized induction heating, *Compos Sci. Technol.*, 63 (15) (2003) 2201-2215.

[10] R. Johnson and R. Pitchumani, Flow control using localized induction heating in a VARTM process, *Compos Sci Technol*, 67 (3-4) (2007) 669-684.

[11] D. Bender, J. Schuster and D. Heider, Flow rate control during vacuum-assisted resin transfer molding (VARTM) processing, *Compos Sci Technol*, 66 (13) (2006) 2265-2271.

[12] N. Correia, F. Robitaille, A. C. Long, C. D. Rudd, P. Šimáček and S. G. Advani, Use of resin transfer molding simulation to predict flow, Saturation, and Compaction in the VARTM Process, *J Fluid Eng-T ASME*, 126 (2) (2004) 210-215.

[13] N. Kuentzer, S. Pavel, S. G. Advani and S. Walsh, Correlation of void distribution to VARTM manufacturing techniques, *Compos Part A-Appl S*, 38 (3) (2007) 802-813.

[14] L. Y. Lin, H. J. Lee, C. E. Hong, G. H. Yoo and S. G. Advani, Preparation and characterization of layered silicate/glass fiber/epoxy hybrid nanocomposites via vacuum-assisted resin transfer molding (VARTM), *Compos. Sci. Technol.*, 66 (13) (2006) 2116-2125.

Sang-Jae Yoon is a research fellow of the Research Institute for Applied Mechanics, Kyushu University, Japan. He received his Dr. Eng. degree from Kyushu University in 2014. His research interests include advanced composite materials, acoustic emission analysis and fracture behavior of engineering materials.

Kazuo Arakawa Kazuo Arakawa is a professor of the Research Institute for Applied Mechanics, Kyushu University, Japan. He received his Dr. Eng. degree from Osaka University in 1982. He stayed at University of Washington as a visiting researcher from 1988-1989. He has published over 200 papers in Japanese and International Journals on solid mechanics including fracture mechanics on polymers and composite materials, dental biomaterials, and impact phenomena of golf balls. He has received many academic awards including the Technology Award, the Best Paper Award from the Japanese Society of Experimental Mechanics and so on.

国際化推進共同研究概要

No.16

タイトル：Development of multi-rotor wind turbine system

研究代表者：JAMIESON, PETER

所内世話人： 大屋 裕二

来訪期間： 2014 年 10 月 15 日 ～ 10 月 24 日

概要：

Prof. Peter Jamieson

エジンバラにあるストラスクライド大学と九州大学応用力学研究所で集風体付き風車とマルチロータ型風車の共同研究を行った。ストラスクライド大学は数値計算により集風体の理想形状を追及している。またマルチロータデザインはヨーロッパの InnWind 計画の一部としても行われ数値計算の結果 7 個のデザインでも 45 個のデザインでも若干の（３％および８％）出力増加をみた。九州大学は数値計算、風葬実験、また野外試験により同じく集風体の効果、またマルチデザインの効果を検証しており、ストラスクライド大学の CFD 計算などのサポートは有意義なものである。

Ducted Wind Turbines and Multi Rotor Systems

University of Strathclyde: Peter Jamieson (67 years, male)

Aim of the collaboration

The collaboration between Kyushu University RIAM and the University of Strathclyde (Glasgow, Scotland) was begun following an Invitation by Professor Yoshida to Peter Jamieson (PJ) to give a presentation (The Development of Wind Energy) at the 10th NCRS International Symposium. During the period around this symposium, in informal workshops hosted by professor Ohya, PJ also received presentations on wind turbine related work at Kyushu and presented work on ducted rotors and on multi rotor systems. The ducted rotor work was of direct relevance to Kyushu as professor Ohya's group had developed the Wind Lens ducted turbine and the multi rotor concept was also of interest because among other potential benefits it offered a means of upscaling net turbine capacity of the Wind Lens without some of the problems in constructing a single large ducted rotor. Thus a collaboration was established with the aims:

a) To exchange information regarding especially the experimental developments of the Wind Lens at Kuyshu related to analytical work on ducted rotors at Strathclyde
b) To jointly explore the multi rotor concept again involving interaction between small scale experiments at Kyushu with large scale system design and analysis work at Strathclyde associated with Innwind.EU, a European collaborative project.

Method

Following the initial meeting (November –December 2013) at the 10th NCRS International Symposium, Uli Göltenbott, a student at Kyushu with Prof. Ohya commenced a PhD study relating to Wind Lens in the context of multi rotor systems. Some experiments were completed within a few months of the initial contact in December 2013. Later in June 2014, Professor Ohya and Dr Nagai visited Strathclyde University (June13th 2014) when further presentations were exchanged and an agreement to collaborate was consolidated. Prof. Ohya had obtained funding to support a further visit to Kyushu by PJ and Scott McLaren-Gow, at student at Strathclyde University now nearing completion of a 4 year PhD working on ducted rotor design and this visit took place from 20th to 24th October 2014. Following this meeting specific information on the Wind Lens configuration was provided to Strathclyde University and on multi rotor systems to Kyushu.

Results and discussion

The findings of the University of Strathclyde are primarily reported here. It is expected that the related work at Kyushu RIAM will be further detailed in other reports. Within the Innwind project, CFD by the University of Athens (within the Innwind EU project in which PJ led a study of the multi rotor concept) has shown small power gains ~ 3% for a 7 rotor array (6 six rotor symmetrically disposed around a central rotor all at 5% diameter minimum distance apart). By power gain is meant more power from the 7 rotor array than 7 x power of a single rotor operating in isolation. Similar CFD analysis of a 45 rotor array showed an augmented power gain of ~ 8% (at 5% and 2.5% diameter minimum rotor spacings). Supplementary analyses showed that for bare rotors without ducts such power gains were

substantially realised at closest possible spacings and that flow in the spaces between the rotors was important to achieve the power augmentation. Related experimental work at RIAM on a ducted, 3 rotor, multi rotor array showed power gains providing there was a sufficient spacing between rotors.

The PhD of Scott McLaren-Gow at Strathclyde University in the Centre for Doctoral Training in Wind Energy has a focus is on getting a much deeper understanding of fundamentals of ducted rotor systems primarily based on inviscid flow modelling using well established panel methods in this case based on a vortex ring representation of the wake. This work is supervised jointly by PJ and Prof. Graham from Imperial College, London who is a world class expert with extensive experience in analysis and numerical modelling of fluids. There appear to be two classes of ducts; those which, loosely speaking, create smoothest flow conditions and may tend to maximise rotor loading at Ct =8/9 and those which induce the largest through flow and highest performance coefficient. Curiously although the detailed mechanisms must be quite different, considering the strong vortex shedding in the CFD modelling at RIAM, the inviscid analyses suggests a broadly similar shape to Wind Lens as optimum. A part of the results is published in the paper as follows,

S. McLaren-Gow, P. Jamieson, and J. Graham, "Ducted turbine theory with right angled ducts," in Journal of Physics: Conference Series, 2014, p. 012083.
The full paper can be obtained here, http://iopscience.iop.org/1742-6596/524/1/012083

A key issue where Strathclyde may be able to assist RIAM is in the optimisation of the rotor which in general is different in ducted operation as compared with open flow. Of course this can and should be supported by CFD but the rotor design optimisation needs some guidance from theory to be an efficient process.

国際化推進共同研究概要

No.17

タイトル：Investigation on wake interaction of wind turbines with relatively small spacing

研究代表者：KOYAMA, Ye-Bonne, Karina

所内世話人： 大屋 裕二

来訪期間： 2014 年 6 月 9 日 ～ 6 月 12 日

概要：

Ye-Bonne Koyama 報告書概要

九州大学のサポートによってハンブルグで行われた CWE2014 学会に参加した。学会では応用力学研究所でインターンとして行った三角形にアレンジされた 3 基の風車周りの流れの研究について発表した。鳥が編隊を組んで飛ぶ場合「V」型に並ぶがそのような工夫で 3 基の風車の配置を考えるとさらに発電効率が上がるのでは、などの意見があった。

九州大学
KYUSHU UNIVERSITY

CWE 2014

Report : Computational Wind Engineering conference (CWE) 2014

Hamburg, Germany, June 9th-12th

Ye-Bonne KOYAMA

Thanks to the support given by Kyushu University, I had the opportunity to participate in the CWE 2014 international conference, and give a presentation on the topic : « Flow pattern around three wind turbine generators (WTGs) in a triangular configuration ».
The conference gathered researchers from all around the world, with a large participation of PhD students, who amounted to one third of the presenters. The conference dealt with varied subjects such as meteorology, wind energy, fluid / structure interaction, CFD model development etc… It was very interesting for me to get an awareness of the research that is undergoing worldwide, in all those domains.
In this report I will focus on remarks that were made on my presentation, and on results from other presentations that caught my attention.

➢ Remarks on my presentation

During the question session at the end of my presentation, I was not asked specific questions; rather, I received quite relevant remarks:

- It could be interesting to have an idea of the *load on the downstream WTGs*. The load on the WTGs in the downstream could be higher than that on the first row, because of a higher wind velocity in front of their blades. Also, when there is a storm, the gap flow between the WTGs of the first row could induced important loads on the second row of WTGs. Prof. Stefan Emeis mentioned that there has been a case when a storm hit a wind farm and only WTGs of the second row collapsed.

- An original remark: when the birds fly in the sky, they tend to form a "V" shape. This shape enables to diminish their energy consumption thanks to the influences of the wakes of the upstream birds on the downstream ones (downstream birds can benefit from the ascending part of the vortices created on the wings of the bird in their upstream). There is an optimal angle for the "V" shape used by birds. Consequently, there could be an optimal angle also for our triangular structure.

- According to our study, we can deduce the following: if we can place obstacles in the upstream of a WTG in an appropriate way, it could generate an increase in the power output of this WTGs (thanks to the phenomena that we have shown)

Due to those remarks and to later discussions with people attending my presentation, I believe that the attendance was interested in my subject, and were quite convinced that this could work.

➢ **Some presentations that caught my attention**

Please find attached the full articles for those presentations.

- Marcel VOLANTHEN gave a presentation on nested LES. The goal is to do CFD on a coarser grid (for example if a large area has to be meshed, such as an urban area), and nest a finer grid inside this coarser grid. The advantage of nested LES compared to local refinement is that the time-step can be different on the finer gird than on the coarser grid, which saves computational time. In order for the energy spectrum to have the appropriate resolution, synthetic turbulent fluctuations are added to the coarse-grid solution at the interface between the fine and coarse grid.

- Yingli XUAN gave a presentation on the way to generate appropriate boundary conditions, especially when we want to use data from a larger-scale model for a smaller scale model. Her work dealt with the way to artificially add fluctuations (that verify properties of turbulence) to the solutions of larger-scale models and use those as inflow boundary conditions for smaller scale models. However those artificial fluctuations can easily be damped away because they do not verify the continuity condition. Yingli XUAN developed a method to ensure that those fluctuations verify the continuity condition.

- R. LÖHNER gave a keynote lecture on the fundamental physical differences between traditional aerospace problems and computational wind engineering (CWE) problems. He studies the influence of the wind on lightweight structures such as umbrellas. He talked about a surprising fact: he ran the same calculations on different numbers of processors; for a moment, the results of all the calculations are the same, but they start to diverge afterwards. Consequently, he stressed the fact that it is very important to run long simulations, run several times the same calculation on different numbers of processors, and analyse the results statistically. Also, he mentioned the adjoint solvers that enable to tell the sensitivity of the calculations to the boundary conditions or the obstacle's geometry.

- Paolo SCHITO presented a new actuator line model for wind turbines, which would not be based on the blade element theory, but an effective velocity method. This enables to take into account shear or turbulence on the blades.

- Tomo's presentation.

➢ **Conclusion**

I was really happy to attend CWE 2014, and represent our team in Germany.
I hope that the research linked to triangular configurations of WTGs is going to continue at Kyushu University.
Please do not hesitate to ask me if you need more details / reporting on the conference.
ありがとうございました